

Supporting Information

NHC Copper(I) Complexes Bearing Dipyridylamine Ligands: Synthesis, Structural and Photoluminescent Studies.

R. Marion,^a F. Sguerra,^b F. Di Meo,^c E. Sauvageot,^a J.-F. Lohier,^a R. Daniellou,^d J.-L. Renaud,^a M. Linares,^{c,*} M. Hamel,^{b,*} S. Gaillard^{a,*}

Table of Content

| | |
|---|---------|
| Part 1: Synthesis of copper complexes 15-18 and 22 | S3-S5 |
| Part 2: Synthesis of ligands L6 ó L9 | S6-S7 |
| Part 3: Crystallographic data of [Cu(NHC)(N [^] N)][X] complexes | S9-S11 |
| Part 4: Photophydic properties of [Cu(NHC)(N [^] N)][X] complexes | S12-S14 |
| Part 5: Voltammogram of [Cu(NHC)(N [^] N)][X] complexes | S15-S17 |
| Part 6: Additional DFT studies on [Cu(NHC)(N [^] N)][X] complexes | S18-S22 |
| Part 7: ¹ H and ¹³ C NMR spectra of compounds | S23-S60 |

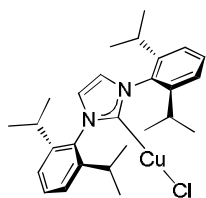
General Considerations. All reactions were carried out using standard Schlenk technique under an atmosphere of dry Argon. Imidazolium chloride salts, 4,5-dihydroimidazolium chloride salts and N⁺N ligands were purchased from commercial sources. Solvents were purchased from Carlo Erba and degassed prior to use by bubbling argon gas directly in the solvent. Solvents for NMR spectroscopy were dried over molecular sieves. NMR spectra were recorded on a 400 MHz and 500 MHz Brücker spectrometers. Proton (¹H) NMR information is given in the following format: multiplicity (s, singlet; d, doublet; t, triplet; q, quartet; qui, quintet; sept, septet; m, multiplet), coupling constant(s) (*J*) in Hertz (Hz), number of protons. The prefix *app* is occasionally applied when the true signal multiplicity was unresolved and br indicates the signal in question broadened. Carbon (¹³C) NMR spectra are reported in ppm () relative to residual CHCl₃ (77.0) unless noted otherwise. HRMS analyses were performed by LCMT analytical services. NMR solvent was passed through a pad of basic alumina before uses.

Part 1: Synthesis of copper complexes

General Procedure for the Synthesis of [CuCl(NHC)] complexes.¹

In a dry flamed Schlenk tube under argon atmosphere, imidazolium chloride salt (1 eq.) and copper oxide (0.65 eq.) were dissolved in distilled toluene and heated under reflux for 24 h. After cooling down to RT, the mixture was dissolved in dichloromethane and filtered through a silica pad. The filtrate was evaporated to dryness and the product was obtained as a white powder without any further purification.

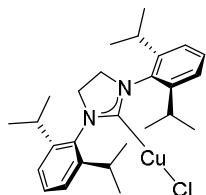
[CuCl(IPr)] (1,3-bis(2,6-di-iso-propylphenyl)imidazol-2-ylidene) copper chloride (**15**)



Following the general procedure, the product was obtained with 81% yield.

¹H-NMR (CDCl₃, 400MHz): δ 1.22 (d, *J* = 6.9 Hz, 12H), 1.30 (d, *J* = 6.8 Hz, 12H), 2.56 (septet, *J* = 6.8 Hz, 4H), 7.13 (s, 2H), 7.30 (d, *J* = 7.8 Hz, 4H), 7.49 (t, *J* = 7.8 Hz, 2H) ppm.

[CuCl(SIPr)] (1,3-bis(2,6-di-iso-propylphenyl)-4,5-dihydroimidazol-2-ylidene) copper chloride

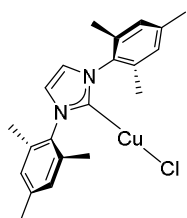


Following the general procedure, the product was obtained with 75% yield.

¹H-NMR (CDCl₃, 400MHz): δ 1.34 (d, *J* = 7.0 Hz, 12H), 1.37 (d, *J* = 7.0 Hz, 12H), 3.07 (septet, *J* = 6.8 Hz, 4H), 4.02 (s, 4H), 7.24 (d, *J* = 8.0 Hz, 4H), 7.40 (t, *J* = 7.8 Hz, 2H) ppm.

¹ a) Citadelle, C. A.; Le Nouy, E.; Bisaro, F.; Slawin, A. M. Z.; Cazin, C. S. J. *Dalton Trans.* **2010**, *39*, 4489-4491. b) Santoro, O.; Collado, A.; Slawin, A. M. Z.; Nolan, S. P.; Cazin, C. S. J. *Chem. Commun.* **2013**, *49*, 10483-10485.

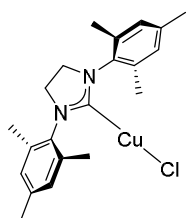
[CuCl(IMes)] (1,3-bis(2,4,6-trimethyl)-imidazol-2-ylidene) copper chloride (**16**)



Following the general procedure, the product was obtained with 79% yield.

¹H-NMR (CDCl₃, 400MHz): δ 2.10 (s, 12H), 2.35 (s, 6H), 7.00 (s, 4H), 7.05 (s, 2H) ppm.

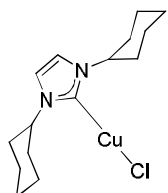
[CuCl(SIMes)] (1,3-bis(bis(2,4,6-trimethyl)-4,5-dihydroimidazol-2-ylidene) copper chloride



Following the general procedure, the product was obtained with 64% yield.

¹H-NMR (CDCl₃, 400MHz): δ 2.30 (s, 6H), 2.32 (s, 12H), 3.95 (s, 4H), 6.95 (s, 4H) ppm.

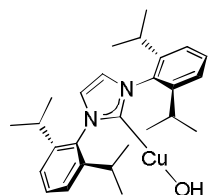
[CuCl(ICy)] (1,3-bis(cyclohexyl)-imidazol-2-ylidene) copper chloride (**17**)



Following the general procedure, the product was obtained as a white solid with 33% yield.

¹H-NMR (CDCl₃, 400 MHz): δ 1.18-1.27 (m, 2H), 1.39-1.51 (m, 4H), 1.29-1.77 (m, 6H), 1.87-1.90 (m, 4H), 2.06-2.09 (m, 4H), 4.29 (tt, *J* = 12.0 Hz et *J* = 4.0 Hz, 2H), 6.92 (s, 2H) ppm.

[CuOH(IPr)] (1,3-bis(2,6-di-*iso*-propylphenyl)imidazol-2-ylidene) copper hydroxide (**18**)²



In a dry flamed Schlenk tube under argon atmosphere, [CuCl(IPr)] (1.3 g, 1 eq.) and CsOH (0.90 g, 2 eq.) were introduced in dry degassed THF. The mixture was allowed to stir at room temperature for 20 hours. After filtration on a pad of celite®, pentane was added to the filtrate and the resulting precipitate was collected on a frit. The solid was then dissolved in toluene to filter off a brownish residue. After concentration of the filtrate, pentane was added and the resulting precipitate was collected on a frit and dried under *vacuum*. The product was obtained as a white solid (0.83 g, 66%).

¹H-NMR (CDCl₃, 400 MHz): δ 1.22 (d, *J* = 6.8 Hz, 12H), 1.31 (d, *J* = 6.8 Hz, 12H), 2.57 (sept, *J* = 6.8 Hz, 4H), 7.10 (s, 2H), 7.29 (d, *J* = 8.0 Hz, 4H), 7.48 (t, *J* = 7.6 Hz, 2H) ppm.

Synthesis of [Cu(IPr)(4,4 ϕ -di-*tert*-butyl-2,2 ϕ -bipyridine)][PF₆] (22)

In a flame-dried Schlenk tube under argon atmosphere, [CuCl(IPr)] complex (**15**) (1 eq.) and 4,4 ϕ -di-*tert*-2,2 ϕ -bipyridine (1.05 eq.) were dissolved in degassed absolute ethanol and heated to reflux for one hour. After cooling to RT, a saturated aqueous solution of KPF₆ was added affording a white precipitate. The solid was washed with water, diethyl ether and dried under vacuum. The product was obtained as a pale brown solid with 94% yield.

¹H-NMR (CDCl₃, 400 MHz): 1.07 (d, *J* = 6.9 Hz, 12H), 1.28 (d, *J* = 6.9 Hz, 12H), 1.35 (s, 18H), 2.64 (sept, *J* = 6.9 Hz, 4H), 6.26 (d, *J* = 5.5 Hz, 2H), 7.13 (d, *J* = 5.5 Hz, 2H), 7.35 (s, 2H), 7.49 (d, *J* = 7.8 Hz, 4H), 7.76 (t, *J* = 7.8 Hz, 2H), 7.91 (s, 2H) ppm. ¹³C-NMR (CDCl₃, 100 MHz): 23.6 (qx4), 25.0 (qx4), 28.8 (dx4), 30.3 (qx6), 35.5 (sx2), 117.9 (dx2), 122.9 (dx2), 123.5 (dx2), 124.7 (dx4), 130.6 (dx2), 135.9 (sx2), 146.3 (sx4), 149.4 (dx2), 152.2 (sx2), 164.5 (sx2), 182.9 (s) ppm. HRMS (ESI): *m/z* calcd for C₄₅H₆₀CuN₄[M₀PF₆]⁺: 719.4114; found: 719.4096. IR (neat): 3168, 3143, 2962, 1610, 1471, 1408, 1329, 1059, 845, 826 cm⁻¹.

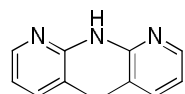
² Fortman, G. C.; Slawin, A. M. Z.; Nolan, S. P. *Organometallics* **2010**, 29, 3966-3972.

Part 2: Synthesis of ligands **L6** ó **L9.**³

General procedure for the synthesis of dipyridylamine derivatives

In a dry flamed Schlenck tube under azote atmosphere, Pd₂(dba)₃ (0.02 eq.) and dppp (0.04 eq.) were dissolved in 25 ml of degased toluene. 2-bromomethylpyridine (1 eq.) was added, followed by 2-aminomethylpyridine (1.2 eq.) and potassium *tert*-butoxide (1.4 eq.) in this order. The mixture was heated at 110°C overnight. After cooling to room temperature, the mixture was filtrate over a pad of celite®. The cake was washed with ethyl acetate. The filtrate was concentrated *in vacuum* to lead to a brown oil. The crude product was purified over column chromatography with pentane/ethyl acetate (2/1).

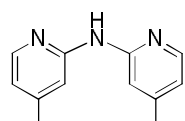
3,3 \bullet dimethyl-2,2 \bullet dipyridylamine (L6)



Following the general procedure, the product was obtained as a white solid with 37% yield.

¹H-NMR (CDCl₃, 400 MHz): δ 2.24 (s, 6H), 6.40-6.51 (*br s*, NH), 6.88 (t, *J* = 6.0 Hz, 2H), 7.46 (d, *J* = 7.3 Hz, 2H), 8.14 (d, *J* = 3.9 Hz, 2H) ppm. ¹³C-NMR (CDCl₃, 100 MHz): δ 18.1 (qx2), 118.0 (dx2), 123.5 (sx2), 138.7 (dx2), 145.4 (sx2), 153.5 (sx2) ppm.

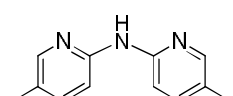
4,4 \bullet dimethyl-2,2 \bullet dipyridylamine (L7)



Following the general procedure, the product was obtained as a white solid with 84% yield.

¹H-NMR (CDCl₃, 400 MHz): δ 2.34 (s, 6H), 6.69 (d, *J* = 5.1 Hz, 2H), 7.36 (s, 2H), 8.12 (d, *J* = 5.1 Hz, 2H) ppm. ¹³C-NMR (CDCl₃, 100 MHz): δ 21.3 (qx2), 111.9 (dx2), 117.7 (dx2), 147.2 (dx2), 149.0 (sx2), 154.2 (sx2) ppm.

5,5 \bullet dimethyl-2,2 \bullet dipyridylamine (L8)

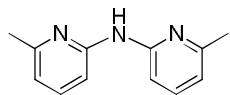


Following the general procedure, the product was obtained as a light brown solid with 77% yield.

³ Sauvageot, E; Marion, R; Sguerra, F.; Grimault, A.; Daniellou, R.; Hamel, M.; Gaillard, S.; Renaud, J.-L. *Org. Chem. Front.* **2014**, *1*, 639-644.

¹H-NMR (CDCl₃, 400 MHz): δ 2.25 (s, 6H), 7.40 (s, 4H), 8.06 (s, 2H) ppm. ¹³C-NMR (CDCl₃, 100 MHz): δ 17.7 (qx2), 111.1 (dx2), 125.1 (sx2), 138.6 (dx2), 147.4 (dx2), 152.2 (sx2) ppm.

6,6 α -dimethyl-2,2 α -dipyridylamine (L9)



Following the general procedure, the product was obtained as a white solid with 90% yield.

¹H-NMR (CDCl₃, 400 MHz): δ 2.45 (s, 6H), 6.68 (d, *J* = 7.6 Hz, 2H), 7.35 (d, *J* = 8.0 Hz, 2H), 7.41-7.46 (*br s*, NH), 7.46 (t, *J* = 8.0 Hz, 2H) ppm. ¹³C-NMR (CDCl₃, 100 MHz): δ 24.3 (qx2), 108.3 (dx2), 115.5 (dx2), 138.0 (dx2), 153.5 (sx2), 156.6 (sx2) ppm.

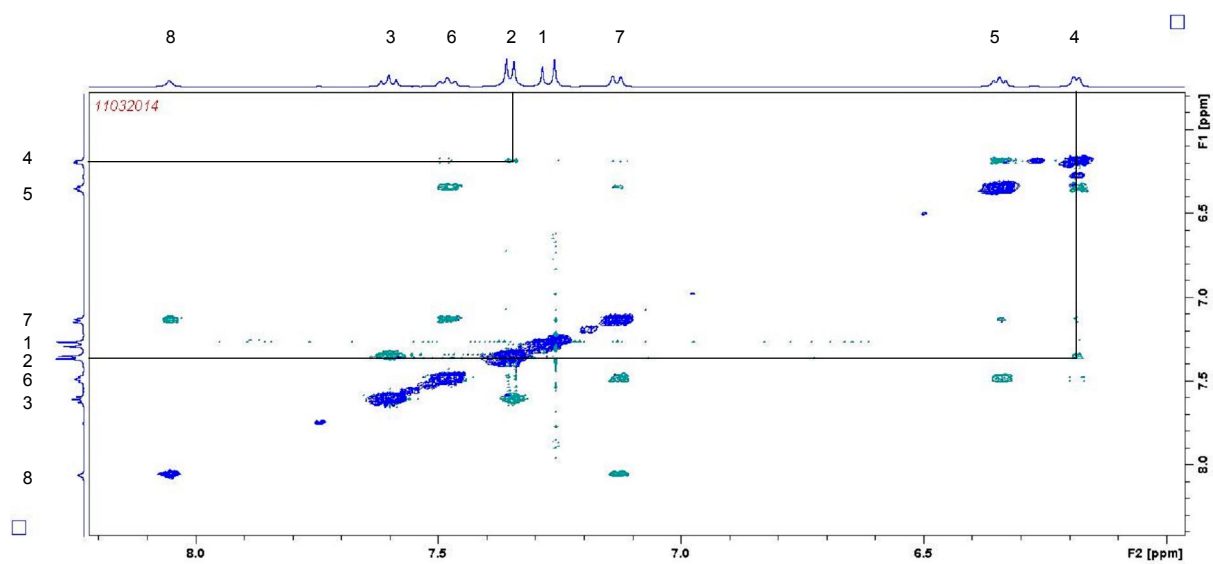
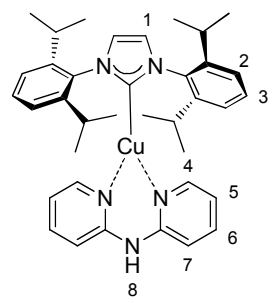


Figure S1. NOESY spectra of complex 5.

Part 3: Crystallographic data of $[\text{Cu}(\text{NHC})(\text{N}^{\text{N}}\text{N})]\text{[X]}$ complexes.

Table S1. Crystallographic data of complexes **4**, **5** and **6**.

| | $[\text{Cu}(\text{IPr})(\text{L4})]\text{[PF}_6\text{] (4)}$ | $[\text{Cu}(\text{IPr})(\text{L5})]\text{[PF}_6\text{] (5)}$ | $[\text{Cu}(\text{IPr})(\text{L6})]\text{[PF}_6\text{] (6)}$ |
|-----------------------------------|--|---|--|
| Formula | $\text{C}_{39}\text{H}_{48}\text{CuF}_6\text{N}_4\text{P}, 2\text{CHCl}_3$ | $\text{C}_{37}\text{H}_{45}\text{CuF}_6\text{N}_5\text{P}, \text{CHCl}_3$ | $\text{C}_{39}\text{H}_{49}\text{CuF}_6\text{N}_5\text{P}$ |
| M/g.mol ⁻¹ | 1020.06 | 887.66 | 796.34 |
| Crystal system | Monoclinic | Orthorhombic | Orthorhombic |
| Flack parameter | | | |
| Space group | <i>P</i> 2 ₁ /c | <i>P</i> na2 ₁ | <i>P</i> bca |
| a/ Å | 9.0406(5) | 12.0145(4) | 16.1394(3) |
| b/ Å | 35.6567(18) | 16.2594(5) | 17.7404(3) |
| c/ Å | 14.9462(7) | 21.7469(7) | 28.0039(5) |
| / ° | - | 90.00 | 90.00 |
| / ° | 101.754(2) | 90.00 | 90.00 |
| / ° | - | 90.00 | 90.00 |
| V/ Å ³ | 4717.0(4) | 4248.2(2) | 8018.1(2) |
| Z | 4 | 4 | 8 |
| calcd/ g.cm ⁻³ | 1.436 | 1.388 | 1.319 |
| $\mu(\text{Mo K})/\text{mm}^{-1}$ | 0.894 | 0.800 | 0.646 |
| T/ K | 150(2) | 150(2) | 291(2) |
| No of reflections | 97907 | 64801 | 166941 |
| No of unique reflections | 13793 | 12313 | 10804 |
| R_{int} | 0.0357 | 0.0252 | 0.0301 |
| $R1, wR2$ (I > 2 (I)) | 0.0547, 0.1420 | 0.0433, 0.1192 | 0.0468, 0.1356 |
| $R1, wR2$ (all data) | 0.0646, 0.1481 | 0.0517, 0.1251 | 0.0682, 0.1537 |
| GOF | 1.029 | 1.041 | 1.027 |

Table S2. Crystallographic data of complexes **8**, **10** and **11**.

| | [Cu(IPr)(L8)][PF ₆] (8) | [Cu(SIPr)(L3)][PF ₆] (10) | [Cu(SIPr)(L5)][PF ₆] (11) |
|---------------------------------|---|---|--|
| Formula | C ₃₉ H ₄₉ CuF ₆ N ₅ P | C ₃₇ H ₄₆ CuF ₆ N ₄ P | C ₃₇ H ₄₇ CuF ₆ N ₅ P, CHCl ₃ |
| M/g.mol ⁻¹ | 796.34 | 755.29 | 889.67 |
| Crystal system | Monoclinic | Orthorhombic | Triclinic |
| Flack parameter | | | |
| Space group | <i>P</i> 2 ₁ /c | <i>P</i> nma | <i>P</i> -1 |
| a/ Å | 11.9827(3) | 14.1077(3) | 11.2079(2) |
| b/ Å | 21.4892(6) | 14.3299(3) | 11.7079(2) |
| c/ Å | 16.9450(5) | 20.8582(5) | 17.1435(4) |
| / ° | - | 90.00 | 86.786(1) |
| / ° | 105.117(1) | 90.00 | 77.690(1) |
| / ° | - | 90.00 | 79.534(1) |
| V/ Å ³ | 4212.3(2) | 4216.73(16) | 2160.95(7) |
| Z | 4 | 4 | 2 |
| calcd/ g.cm ⁻³ | 1.256 | 1.190 | 1.367 |
| μ(Mo K)/ mm ⁻¹ | 0.615 | 0.610 | 0.787 |
| T/ K | 150(2) | 150(2) | 296(2) |
| No of reflections | 52812 | 53196 | 55902 |
| No of unique reflections | 9135 | 5892 | 12644 |
| R _{int} | 0.0273 | 0.0290 | 0.0265 |
| R1, wR ₂ (I > 2 (I)) | 0.0502, 0.1278 | 0.0439, 0.1320 | 0.0492, 0.1259 |
| R1, wR ₂ (all data) | 0.0556, 0.1305 | 0.0524, 0.1370 | 0.0740, 0.1437 |
| GOF | 1.134 | 1.062 | 1.016 |

Table S3. Crystallographic data of complexes **19** and **20**.

| | [Cu(IPr)(L1)][BF ₄] (19) | [Cu(IPr)(L3)][BF ₄] (20) |
|---------------------------------|--|--|
| Formula | C ₃₉ H ₄₄ BCuF ₄ N ₄ | C ₃₇ H ₄₄ BCuF ₄ N ₄ |
| M/g.mol ⁻¹ | 719.13 | 695.11 |
| Crystal system | Monoclinic | Orthorhombic |
| Flack parameter | | |
| Space group | P2 ₁ /c | Pbca |
| a/ Å | 8.8858(3) | 15.3714(3) |
| b/ Å | 22.9533(8) | 16.9525(4) |
| c/ Å | 19.1857(7) | 26.5793(6) |
| / ° | - | 90.00 |
| / ° | 96.252(2) | 90.00 |
| / ° | - | 90.00 |
| V/ Å ³ | 3889.8(2) | 6926.1(3) |
| Z | 4 | 8 |
| calcd/ g.cm ⁻³ | 1.228 | 1.333 |
| μ(Mo K)/ mm ⁻¹ | 0.612 | 0.684 |
| T/ K | 150(2) | 100(2) |
| No of reflections | 31521 | 62682 |
| No of unique reflections | 6866 | 8953 |
| R _{int} | 0.0364 | 0.0248 |
| R1, wR ₂ (I > 2 (I)) | 0.0657, 0.1464 | 0.0426, 0.1148 |
| R1, wR ₂ (all data) | 0.0897, 0.1568 | 0.0520, 0.1186 |
| GOF | 1.034 | 1.069 |

Part 4: Photophysics properties of $[\text{Cu}(\text{NHC})(\text{N}^{\wedge}\text{N})]\text{[X]}$ complexes

UV-visible spectra were measured at room temperature in chloroform on a Jenway 6715 UV/Vis spectrometer, wavelengths are given in nm and extinction coefficients are presented in $\text{L.mol}^{-1}.\text{cm}^{-1}$. Steady-state emission spectra and emission lifetime were recorded on solid state on an Horiba Jobin Yvon Fluoromax-4 spectrofluorometer. For measuring absolute solid-state emission quantum yield, an Horiba Jobin Yvon integrating sphere F-3018 was equipped to the Fluoromax-4 spectrofluorometer.

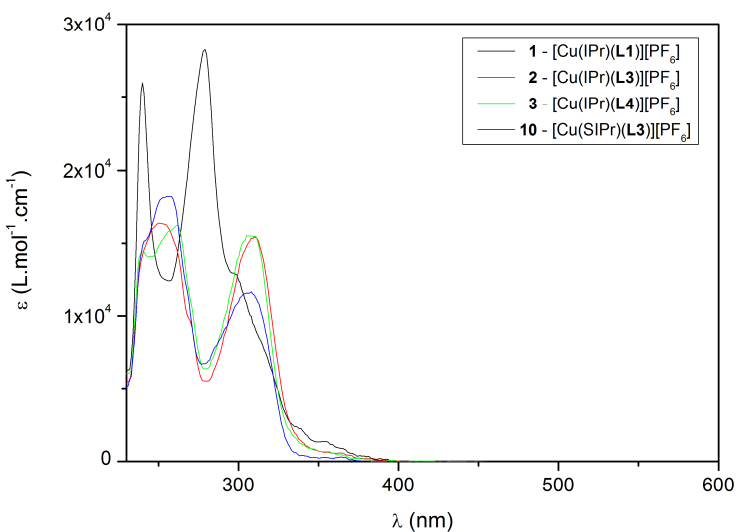


Figure S2. Absorption spectra in CHCl_3 of complexes **1**, **3**, **4** and **10**.

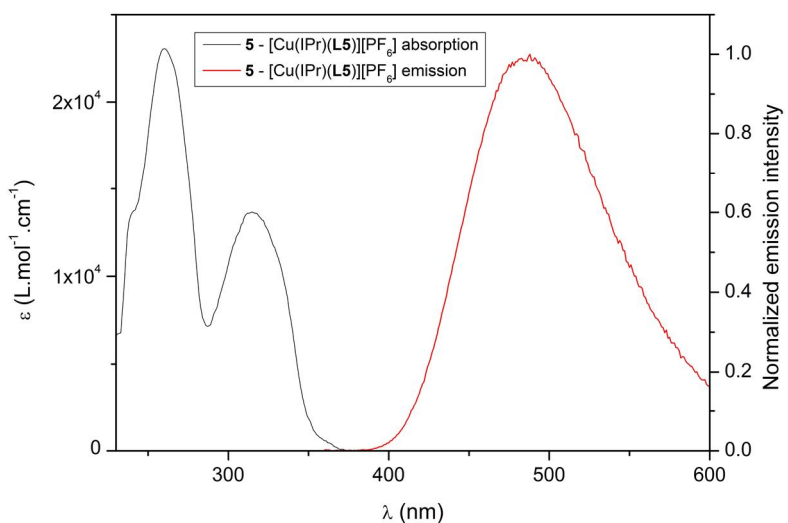


Figure S3. Absorption (in CHCl_3) and emission (in the solid state) spectra of complex **5**.

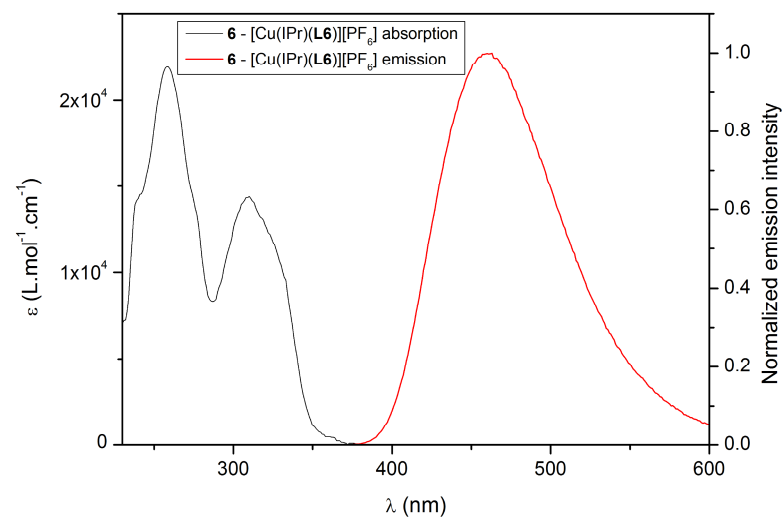


Figure S4. Absorption (in $CHCl_3$) and emission (in the solid state) spectra of complex **6**.

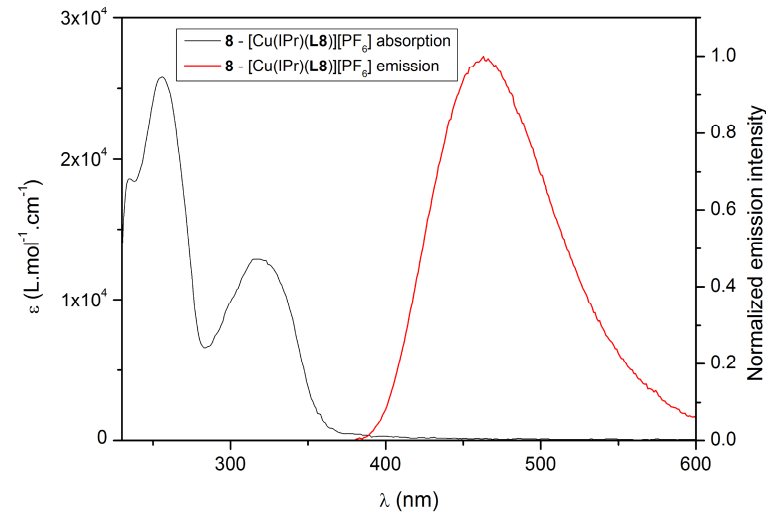


Figure S6. Absorption (in $CHCl_3$) and emission (in the solid state) spectra of complex **8**.

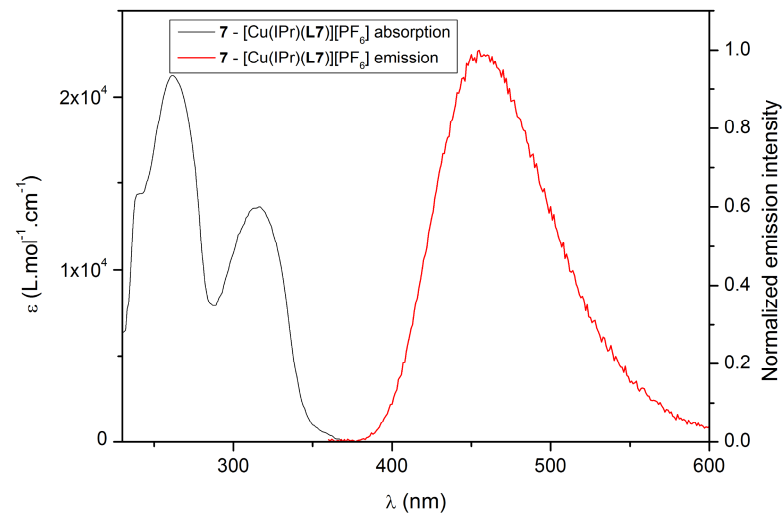


Figure S5. Absorption (in $CHCl_3$) and emission (in the solid state) spectra of complex **7**.

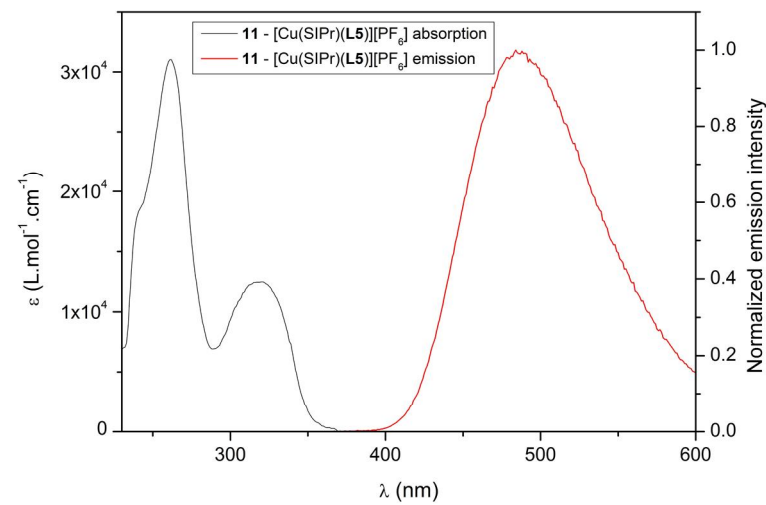


Figure S7. Absorption (in $CHCl_3$) and emission (in the solid state) spectra of complex **11**.

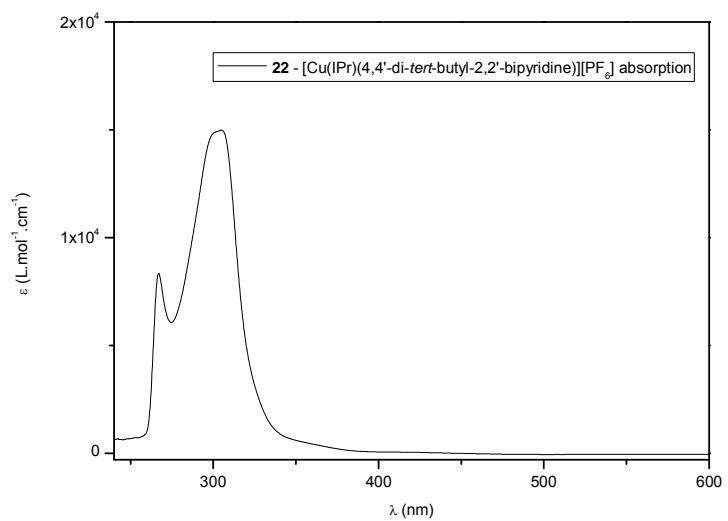


Figure S8. Absorption spectra in CHCl_3 of complex **22**.



Figure S9. Complex **5** (left) and complex **22** (right) under UV irradiation at 366 nm.

Part 5: Voltammogram of $[\text{Cu}(\text{NHC})(\text{N}^{\text{N}})][\text{X}]$ complexes

Voltammetric experiments were carried out using a Biologic potentiostat unit, with the EC-Lab software package. A vitreous carbon working electrode, a platinum wire auxiliary electrode, and a saturated calomel reference electrode (SCE) were used in a standard three-electrode configuration. Cyclic voltammetries were performed in anhydrous dichloromethane, containing 0.1 M tetrabutylammonium hexafluorophosphate, at a 25 mV.s^{-1} scan rate, under a dinitrogen atmosphere.

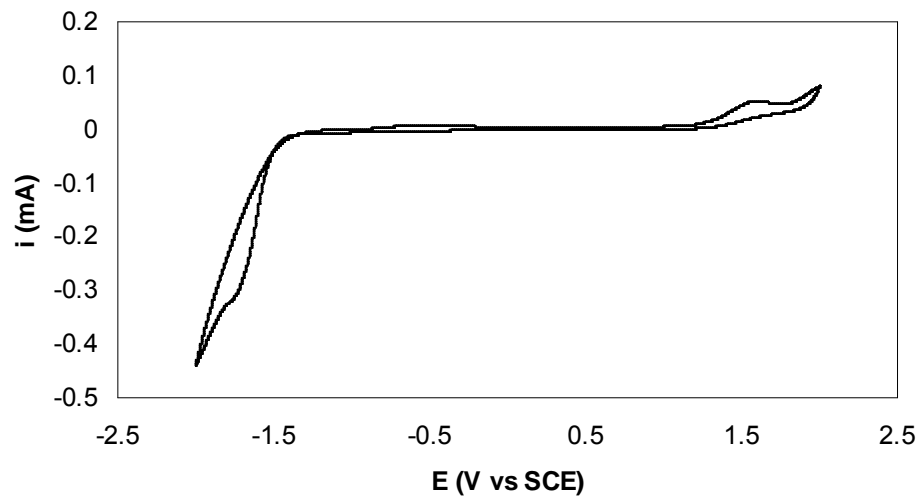


Figure S10. Cyclic voltammogram of complex 1.

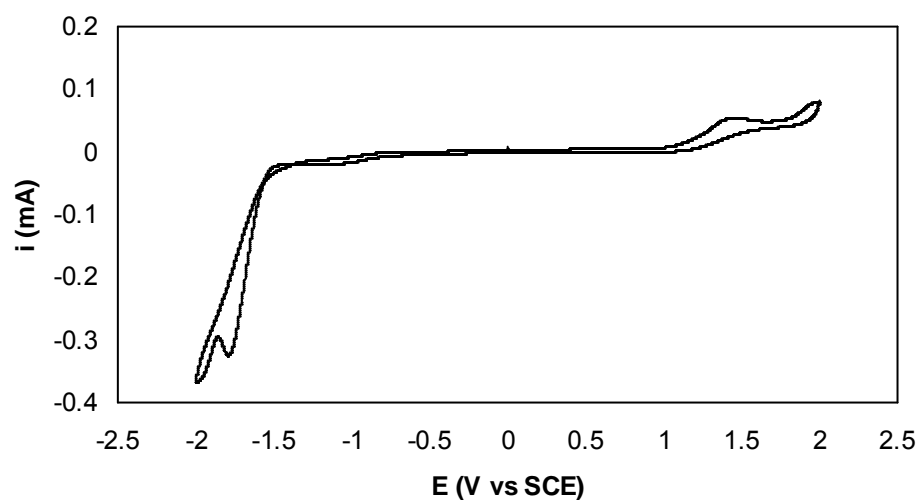


Figure S11. Cyclic voltammogram of complex 3.

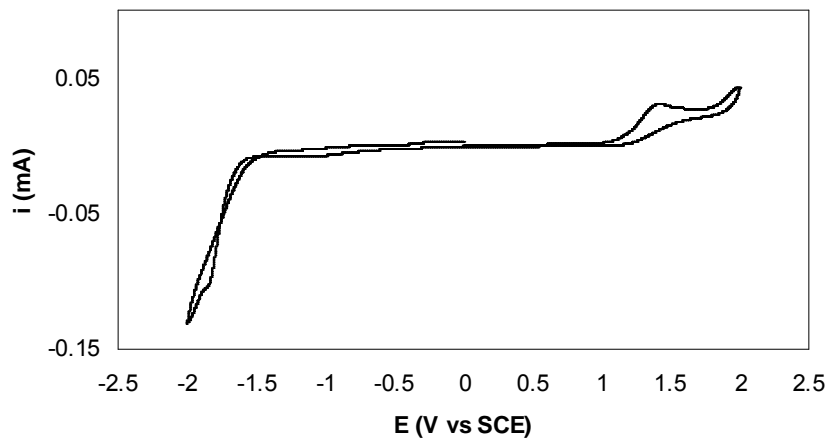


Figure S12. Cyclic voltammogram of complex 4.

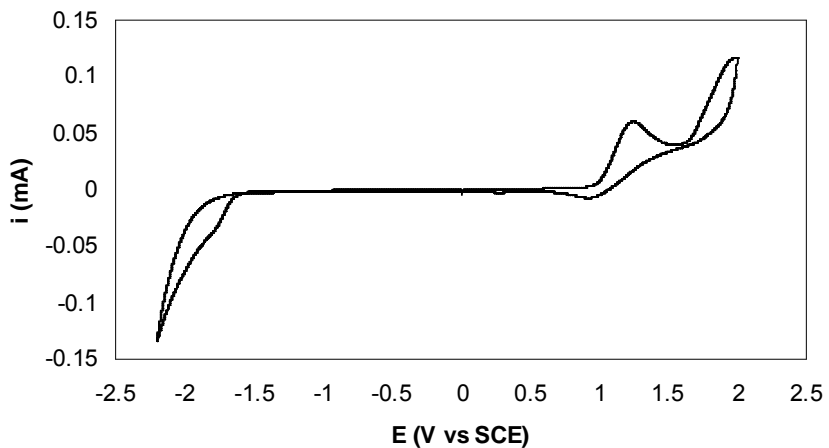


Figure S14. Cyclic voltammogram of complex 6.

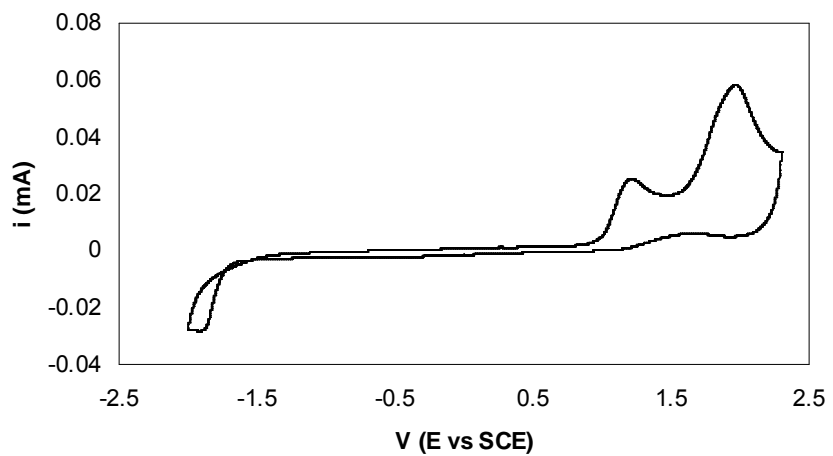


Figure S13. Cyclic voltammogram of complex 5.

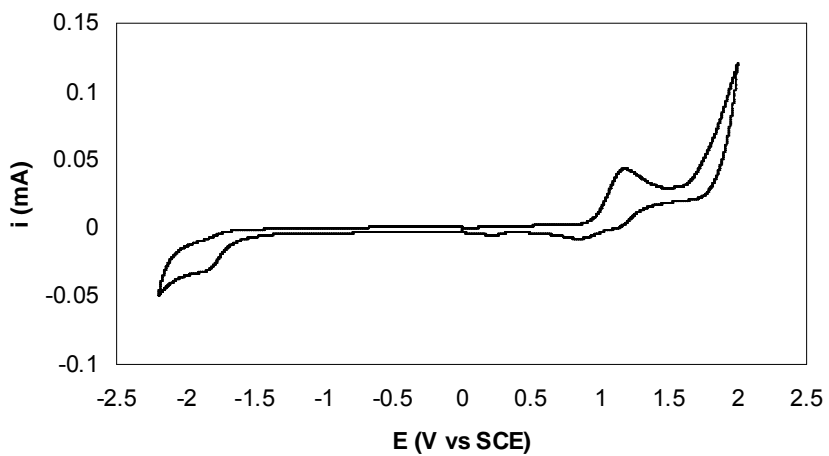


Figure S15. Cyclic voltammogram of complex 7.

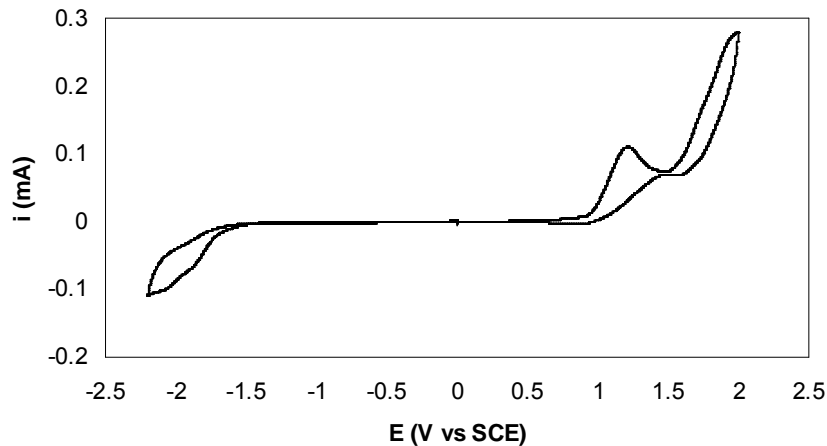


Figure S16. Cyclic voltammogram of complex **8**.

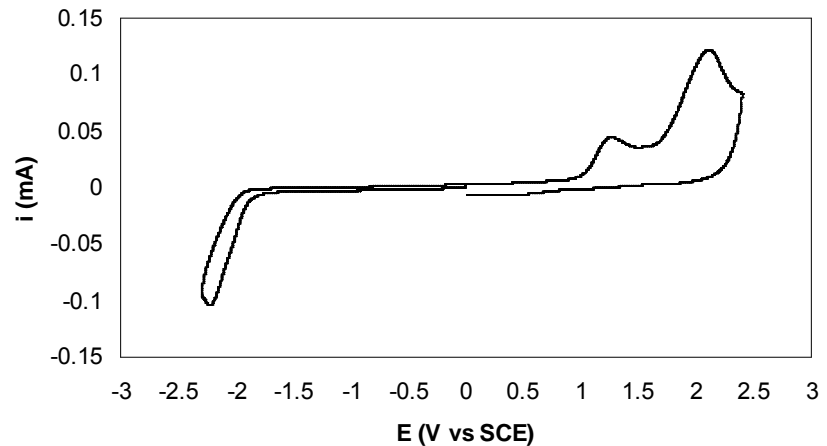


Figure S18. Cyclic voltammogram of complex **11**.

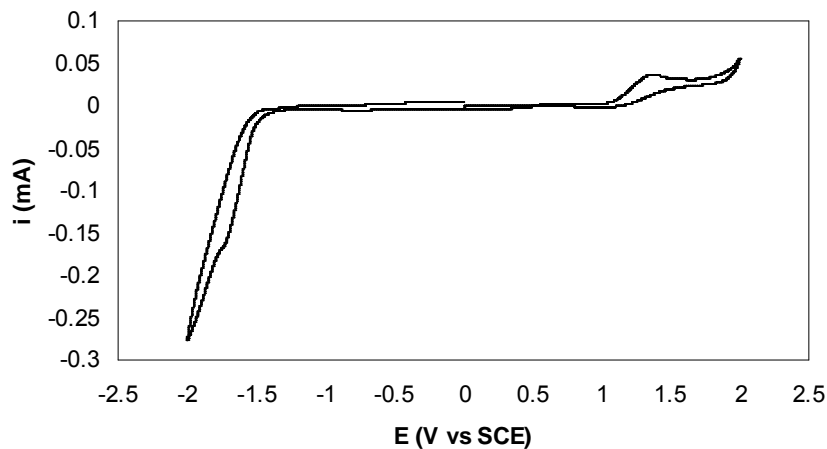


Figure S17. Cyclic voltammogram of complex **10**.

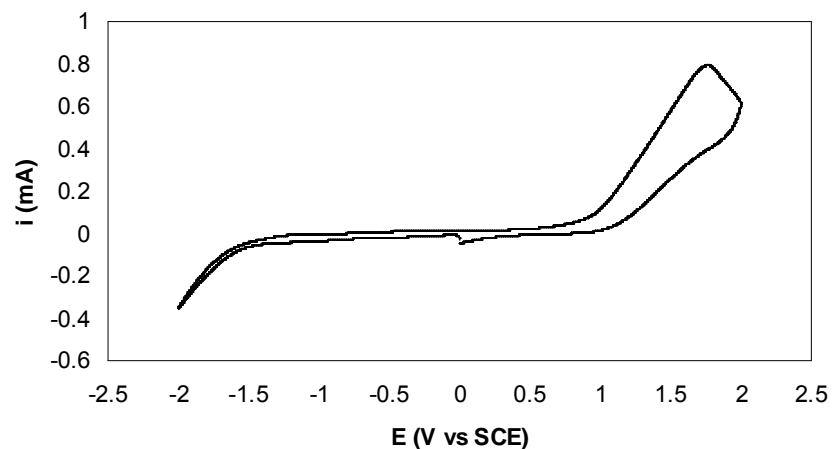


Figure S19. Cyclic voltammogram of ligand (**L5**).

Part 6: Additional DFT studies on [Cu(NHC)(N^N)][X] complexes

Table S4. Bond lengths and angles for the different complexes calculated with the B3LYP functional. The column CH- refers to the distance between the hydrogen and the center of the phenyl ring. C' H' refers to the angle Carbon-Hydrogen-Center of the phenyl ring.

| Complexes | Cu-C _{carbene} (Å) | Cu···N _{ligand} (Å) | N _{ligand} ···Cu···N _{ligand} (°) | N _{ligand} ···Cu···C _{carbene} (°) | CH···π (Å) | C···H···π (°) |
|----------------------------------|--------------------------------|---------------------------------|--|---|---------------|------------------|
| [Cu(IPr)(L1)] ⁺ (1) | 1.915 | 2.118 | 79.310 | 140.345 | 2.697 | 168.338 |
| [Cu(IPr)(L3)] ⁺ (3) | 1.915 | 2.109 | 78.245 | 140.876 | 2.653 | 172.920 |
| [Cu(IPr)(L4)] ⁺ (4) | 1.915 | 2.105 | 78.261 | 140.870 | 2.668 | 172.117 |
| [Cu(IPr)(L5)] ⁺ (5) | 1.932 | 2.112 | 88.216 | 135.776 | 2.698 | 134.257 |
| [Cu(IPr)(L6)] ⁺ (6) | 1.932 | 2.109 | 87.845 | 135.959 | 2.724 | 131.995 |
| [Cu(IPr)(L7)] ⁺ (7) | 1.935 | 2.109 | 88.538 | 135.640 | 2.641 | 137.973 |
| [Cu(IPr)(L8)] ⁺ (8) | 1.932 | 2.114 | 88.343 | 135.622 | 2.879 | 128.733 |
| [Cu(SIPr)(L3)] ⁺ (10) | 1.927 | 2.114 | 78.057 | 140.971 | 2.590 | 173.312 |
| [Cu(SIPr)(L5)] ⁺ (11) | 1.945 | 2.119 | 87.755 | 135.943 | 2.673 | 133.017 |

Table S5. Bond lengths and angles for the different complexes calculated with the M06 functional. The column CH- refers to the distance between the hydrogen and the center of the phenyl ring. C' H' refers to the angle Carbon-Hydrogen-Center of the phenyl ring.

| Complexes | Cu-C _{carbene} (Å) | Cu···N _{ligand} (Å) | N _{ligand} ···Cu···N _{ligand} (°) | N _{ligand} ···Cu···C _{carbene} (°) | CH···π (Å) | C···H···π (°) |
|----------------------------------|--------------------------------|---------------------------------|--|---|---------------|------------------|
| [Cu(IPr)(L1)] ⁺ (1) | 1.898 | 2.087 | 80.343 | 139.828 | 2.550 | 168.522 |
| [Cu(IPr)(L3)] ⁺ (3) | 1.900 | 2.080 | 78.961 | 140.519 | 2.513 | 173.616 |
| [Cu(IPr)(L4)] ⁺ (4) | 1.899 | 2.076 | 79.015 | 140.492 | 2.525 | 172.737 |
| [Cu(IPr)(L5)] ⁺ (5) | 1.912 | 2.076 | 89.237 | 134.845 | 2.630 | 123.461 |
| [Cu(IPr)(L6)] ⁺ (6) | 1.912 | 2.074 | 89.603 | 134.699 | 2.569 | 126.241 |
| [Cu(IPr)(L7)] ⁺ (7) | 1.915 | 2.073 | 89.678 | 134.669 | 2.569 | 127.758 |
| [Cu(IPr)(L8)] ⁺ (8) | 1.913 | 2.077 | 89.144 | 134.885 | 2.783 | 120.887 |
| [Cu(SIPr)(L3)] ⁺ (10) | 1.910 | 2.085 | 78.754 | 140.623 | 2.449 | 173.778 |
| [Cu(SIPr)(L5)] ⁺ (11) | 1.924 | 2.084 | 88.747 | 135.061 | 2.608 | 122.984 |

Energy formation of [Cu(NHC)(N^N)][X] complexes

In order to rationalize our observed results during the synthesis part, energy formation of the copper complexes have also been calculated and are presented in Table S6.

Table S6. Energy formation of copper complexes.

| Complexes | Yield | E(kcal.Mol ⁻¹) |
|-------------------------------------|-------|----------------------------|
| [Cu(IPr)(L1)][PF ₆] (1) | 56 | -73 |
| [Cu(IPr)(L2)][PF ₆] (2) | 0 | -59 |
| [Cu(IPr)(L3)][PF ₆] (3) | 72 | -74 |
| [Cu(IPr)(L4)][PF ₆] (4) | 94 | -77 |
| [Cu(IPr)(L5)][PF ₆] (5) | 72 | -74 |
| [Cu(IPr)(L6)][PF ₆] (6) | 98 | -75 |
| [Cu(IPr)(L7)][PF ₆] (7) | 93 | -76 |
| [Cu(IPr)(L8)][PF ₆] (8) | 73 | -77 |
| [Cu(IPr)(L9)][PF ₆] (9) | 0 | -69 |

| | | |
|---|----|-----|
| [Cu(SIPr)(L3)][PF ₆] (10) | 88 | -75 |
| [Cu(SIPr)(L5)][PF ₆] (11) | 81 | -74 |
| [Cu(IMes)(L5)][PF ₆] (12) | 5< | -72 |
| [Cu(SIMes)(L5)][PF ₆] (13) | 5< | -72 |
| [Cu(ICy)(L5)][PF ₆] (14) | 0 | -66 |

These new results demonstrate that the critical barrier value for the energy formation of this series of copper complexes is located at -72 kcal.mol⁻¹. Indeed, when this energy were found higher for complexes bearing NHC ligand ICy or N⁺N ligands **L2** and **L9**. Then when this energy formation is around -72 kcal.mol⁻¹, reactivity start to be observed but with low conversion. To reach a high conversion into the expected copper this value need to be at least below -74 kcal.mol⁻¹. Of course, these relative values of the energy formation have to be carefully considerate but show clearly the tendency observed on the isolated yields of these copper complexes.

Table S7. HOMO, LUMO level and HOMO-LUMO gap for the different complexes calculated with B3LYP.

| Complexes | HOMO (eV) | LUMO (eV) | HOMO-LUMO gap (eV) |
|---|--------------|--------------|-----------------------|
| [Cu(IPr)(L1)] ⁺ (1) | -8.53 | -4.90 | 3.64 |
| [Cu(IPr)(L3)] ⁺ (3) | -8.53 | -4.95 | 3.59 |
| [Cu(IPr)(L4)] ⁺ (4) | -8.37 | -4.75 | 3.62 |
| [Cu(IPr)(L5)] ⁺ (5) | -8.44 | -4.04 | 4.40 |
| [Cu(IPr)(L6)] ⁺ (6) | -8.31 | -3.90 | 4.41 |
| [Cu(IPr)(L7)] ⁺ (7) | -8.29 | -3.82 | 4.46 |
| [Cu(IPr)(L8)] ⁺ (8) | -8.34 | -3.91 | 4.44 |
| [Cu(SIPr)(L3)] ⁺ (10) | -8.55 | -4.94 | 3.61 |
| [Cu(SIPr)(L5)] ⁺ (11) | -8.47 | -4.03 | 4.44 |

Table S8. HOMO, LUMO level and HOMO-LUMO gap for the different complexes calculated with M06.

| Complexes | HOMO (eV) | LUMO (eV) | HOMO-LUMO gap (eV) |
|---|--------------|--------------|-----------------------|
| [Cu(IPr)(L1)] ⁺ (1) | -9.03 | -4.77 | 4.26 |
| [Cu(IPr)(L3)] ⁺ (3) | -9.03 | -4.81 | 4.21 |
| [Cu(IPr)(L4)] ⁺ (4) | -8.86 | -4.62 | 4.24 |
| [Cu(IPr)(L5)] ⁺ (5) | -8.93 | -3.91 | 5.01 |
| [Cu(IPr)(L6)] ⁺ (6) | -8.80 | -3.80 | 4.99 |
| [Cu(IPr)(L7)] ⁺ (7) | -8.82 | -3.69 | 5.13 |
| [Cu(IPr)(L8)] ⁺ (8) | -8.83 | -3.79 | 5.04 |
| [Cu(SIPr)(L3)] ⁺ (10) | -9.04 | -4.81 | 4.23 |
| [Cu(SIPr)(L5)] ⁺ (11) | -8.95 | -3.90 | 5.05 |

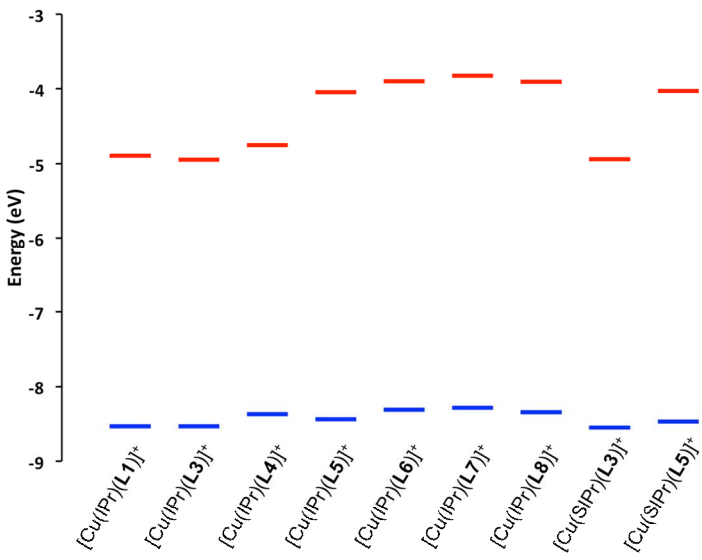


Figure S20. HOMO and LUMO energy diagram for the 9 complexes at the B3LYP level.

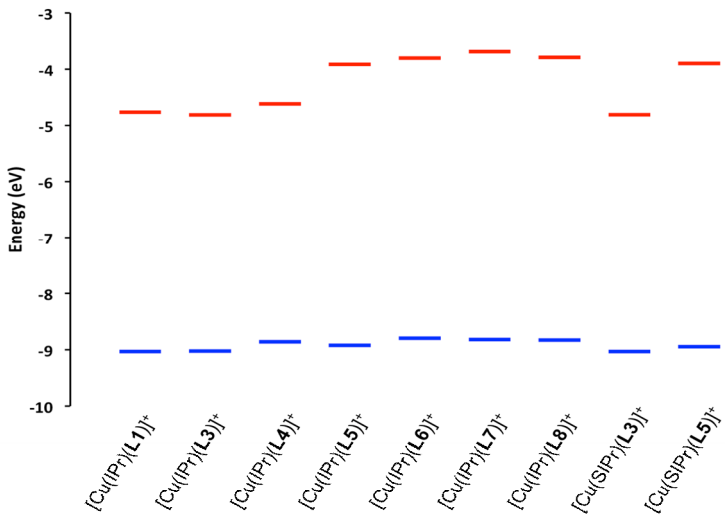


Figure S21. HOMO and LUMO energy diagram for the 9 complexes at the M06 level.

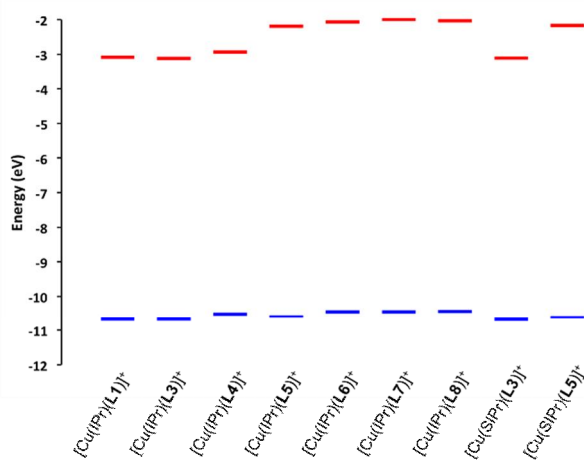


Figure S22. HOMO and LUMO energy diagram for the copper complexes at the B97XD level.

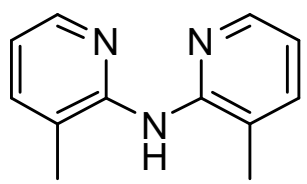
Table S9. Graphic representations of complexes states for S0→S1 transition.

| Complex | S0 → S1 | | Vectors |
|-------------------------------------|---------|----|---------|
| | GS | ES | |
| [Cu(IPr)(L1)] ⁺ (1) | | | |
| [Cu(IPr)(L3)] ⁺ (3) | | | |
| [Cu(IPr)(L4)] ⁺ (4) | | | |
| [Cu(IPr)(L5)] ⁺ (5) | | | |
| [Cu(IPr)(L6)] ⁺ (6) | | | |
| [Cu(IPr)(L7)] ⁺ (7) | | | |
| [Cu(IPr)(L8)] ⁺ (8) | | | |
| [Cu(SIPr)(L3)] ⁺ (10) | | | |
| [Cu(SIPr)(L5)] ⁺ (11) | | | |

Table S10. Graphic representations of complexes states for S0→T1 transition.

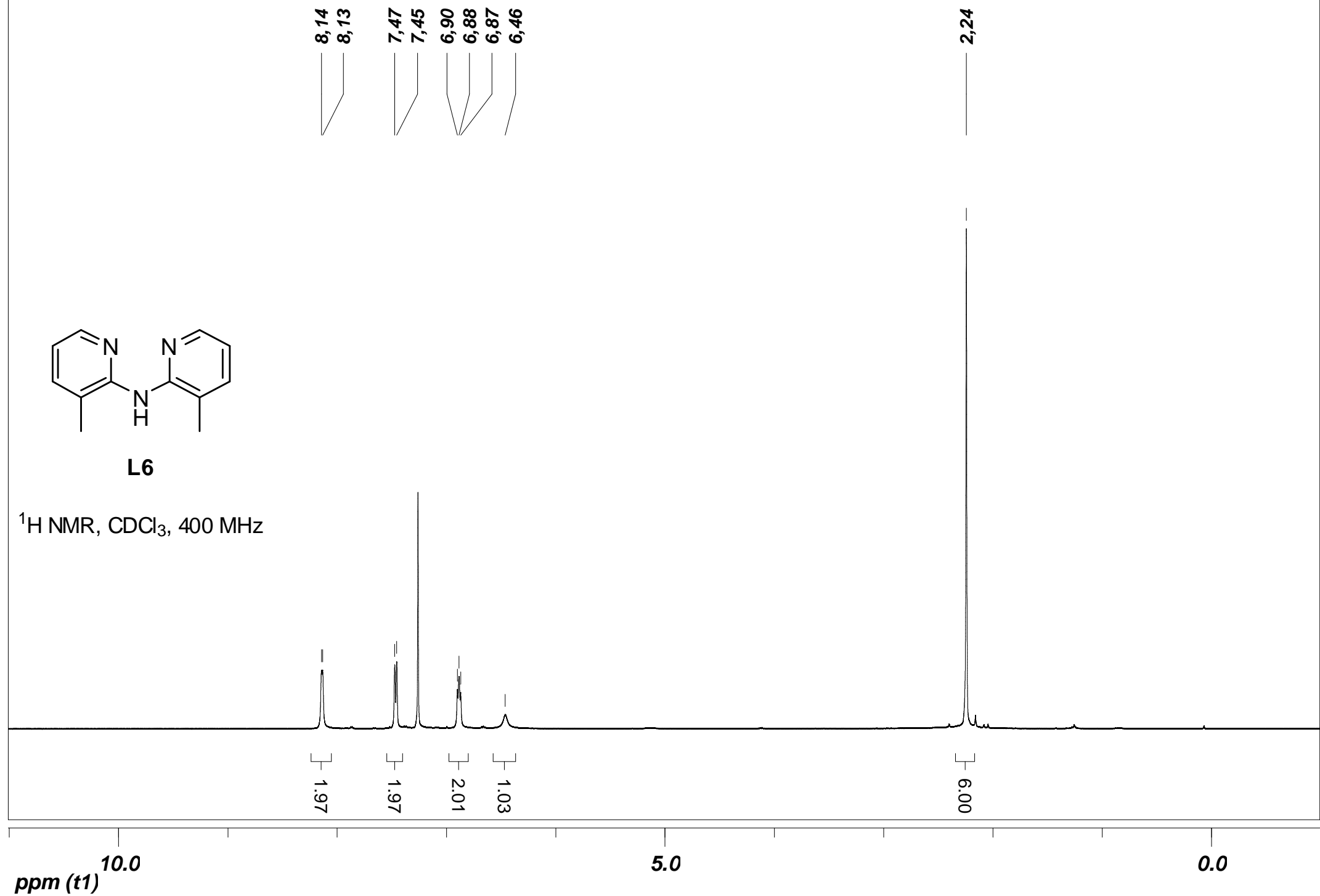
| Complex | S0 → T1 | | Vectors |
|-------------------------------------|---------|----|---------|
| | GS | ES | |
| [Cu(IPr)(L1)] ⁺ (1) | | | |
| [Cu(IPr)(L3)] ⁺ (3) | | | |
| [Cu(IPr)(L4)] ⁺ (4) | | | |
| [Cu(IPr)(L5)] ⁺ (5) | | | |
| [Cu(IPr)(L6)] ⁺ (6) | | | |
| [Cu(IPr)(L7)] ⁺ (7) | | | |
| [Cu(IPr)(L8)] ⁺ (8) | | | |
| [Cu(SIPr)(L3)] ⁺ (10) | | | |
| [Cu(SIPr)(L5)] ⁺ (11) | | | |

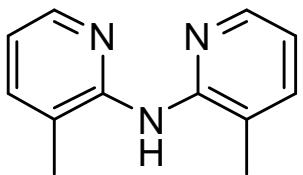
Part 7: ^1H and ^{13}C NMR spectra of compounds



L6

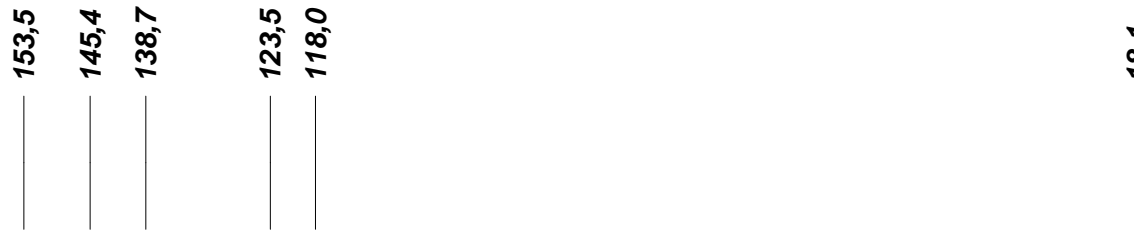
^1H NMR, CDCl_3 , 400 MHz





L6

^{13}C NMR, CDCl_3 , 100 MHz



200

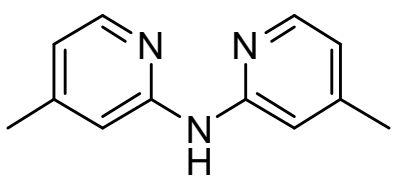
150

100

50

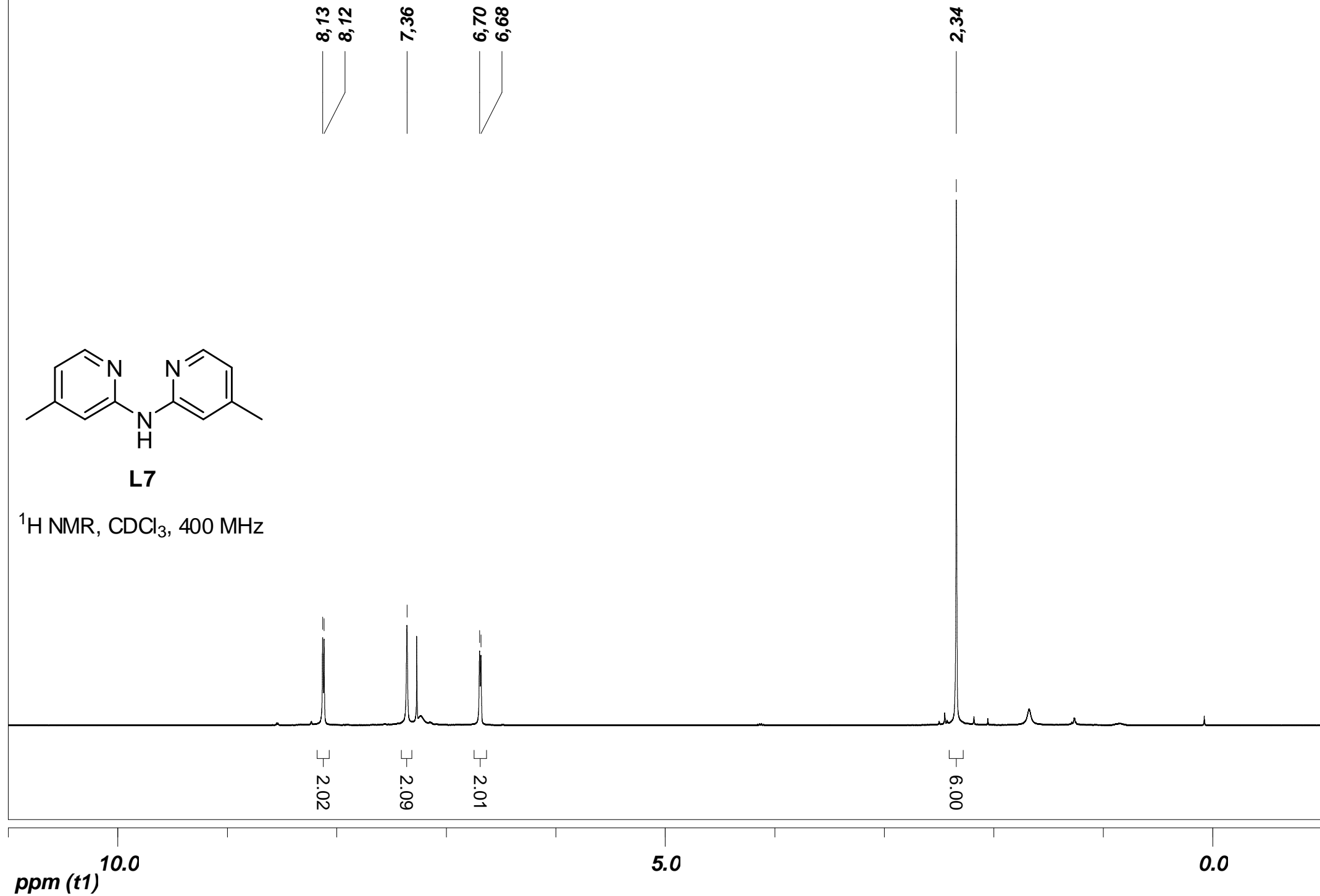
0

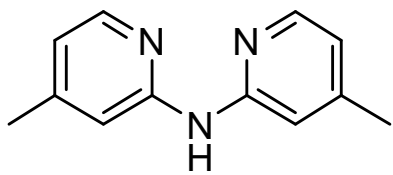
ppm (*t*1)



L7

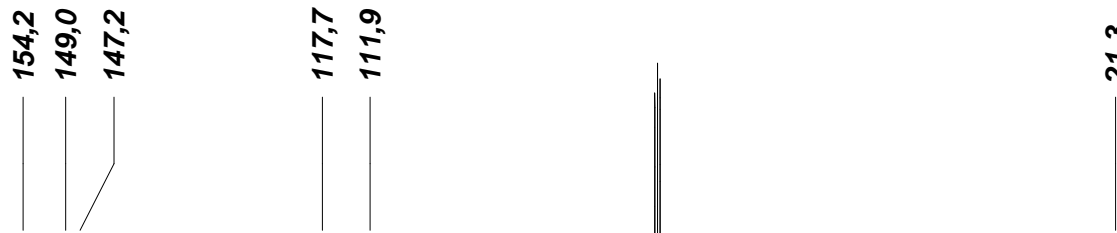
^1H NMR, CDCl_3 , 400 MHz





L7

^{13}C NMR, CDCl_3 , 100 MHz



ppm (t1)

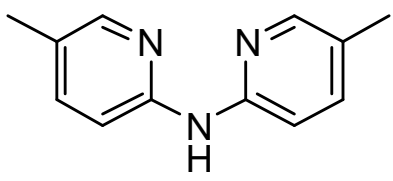
200

150

100

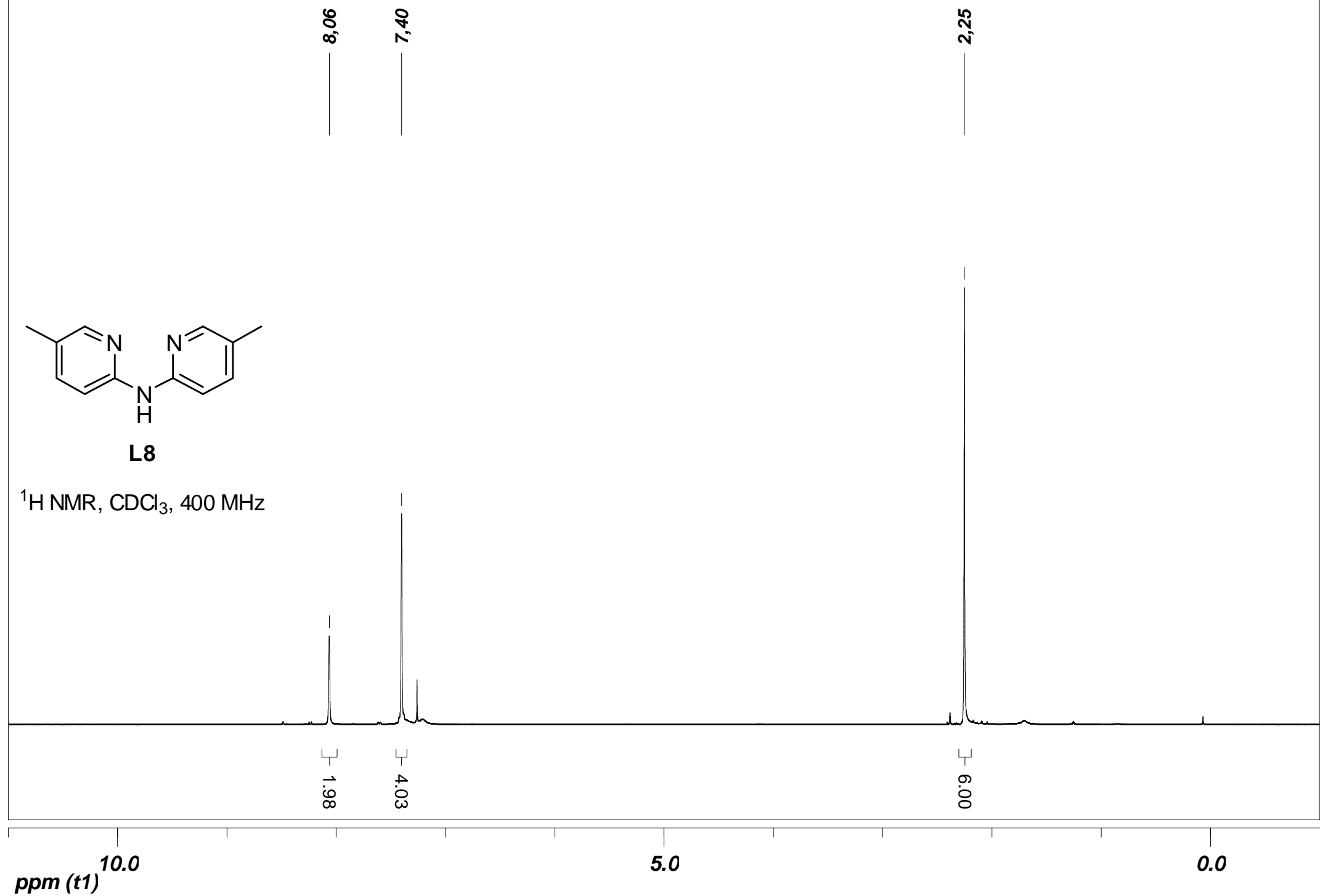
50

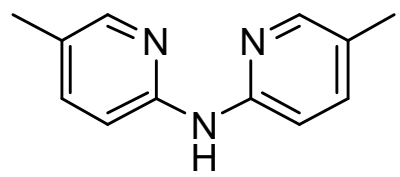
0



L8

^1H NMR, CDCl_3 , 400 MHz





L8

^{13}C NMR, CDCl_3 , 100 MHz



200

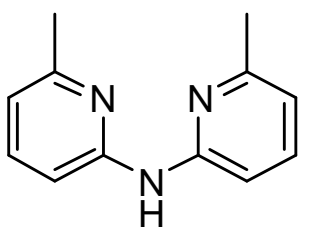
150

100

50

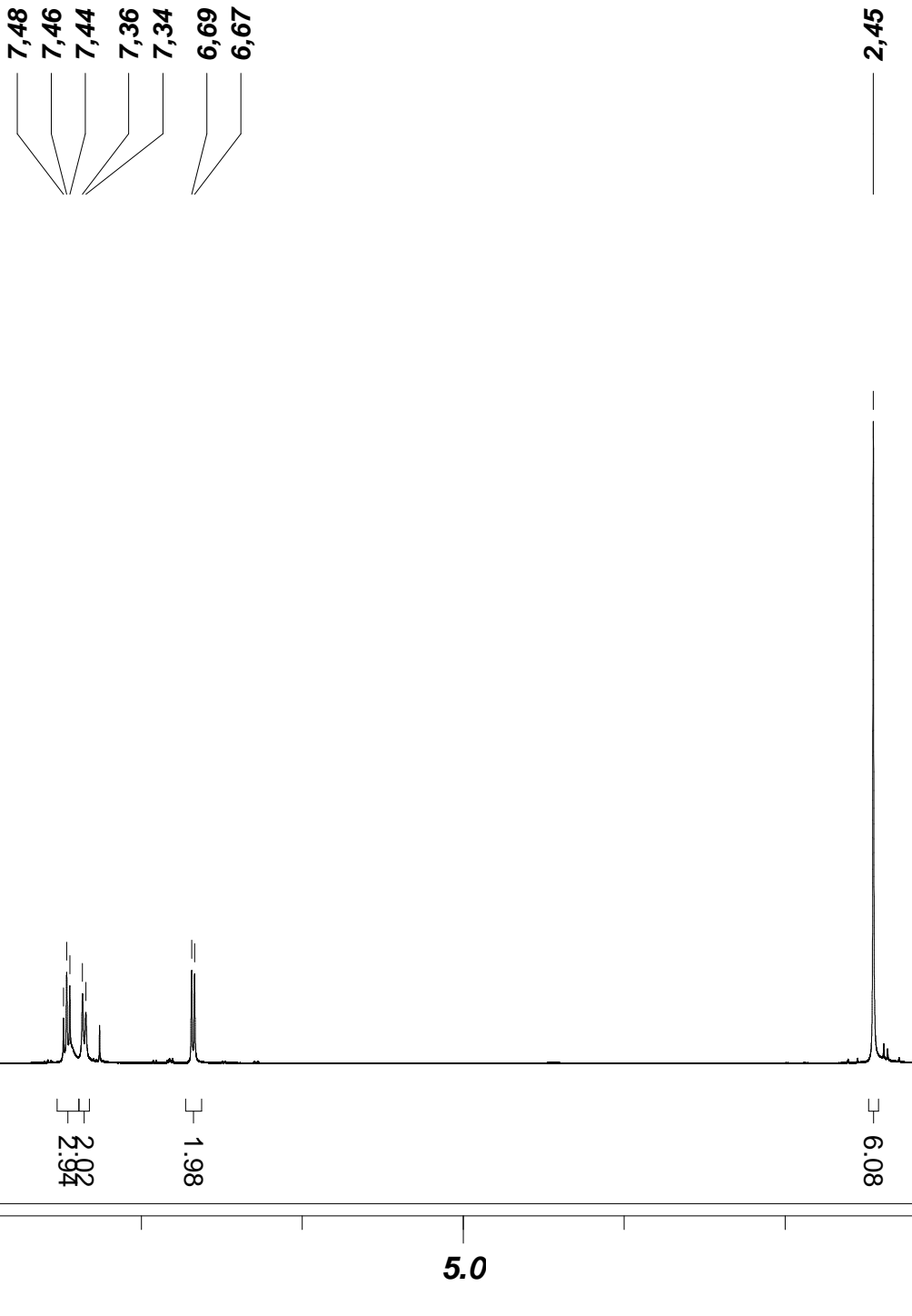
0

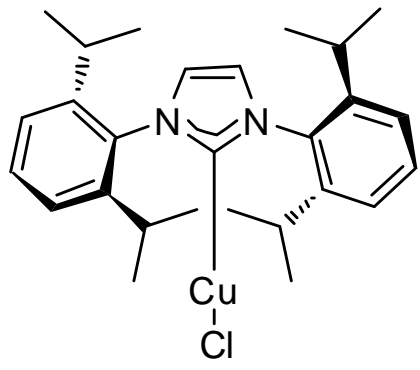
ppm (t1)



L9

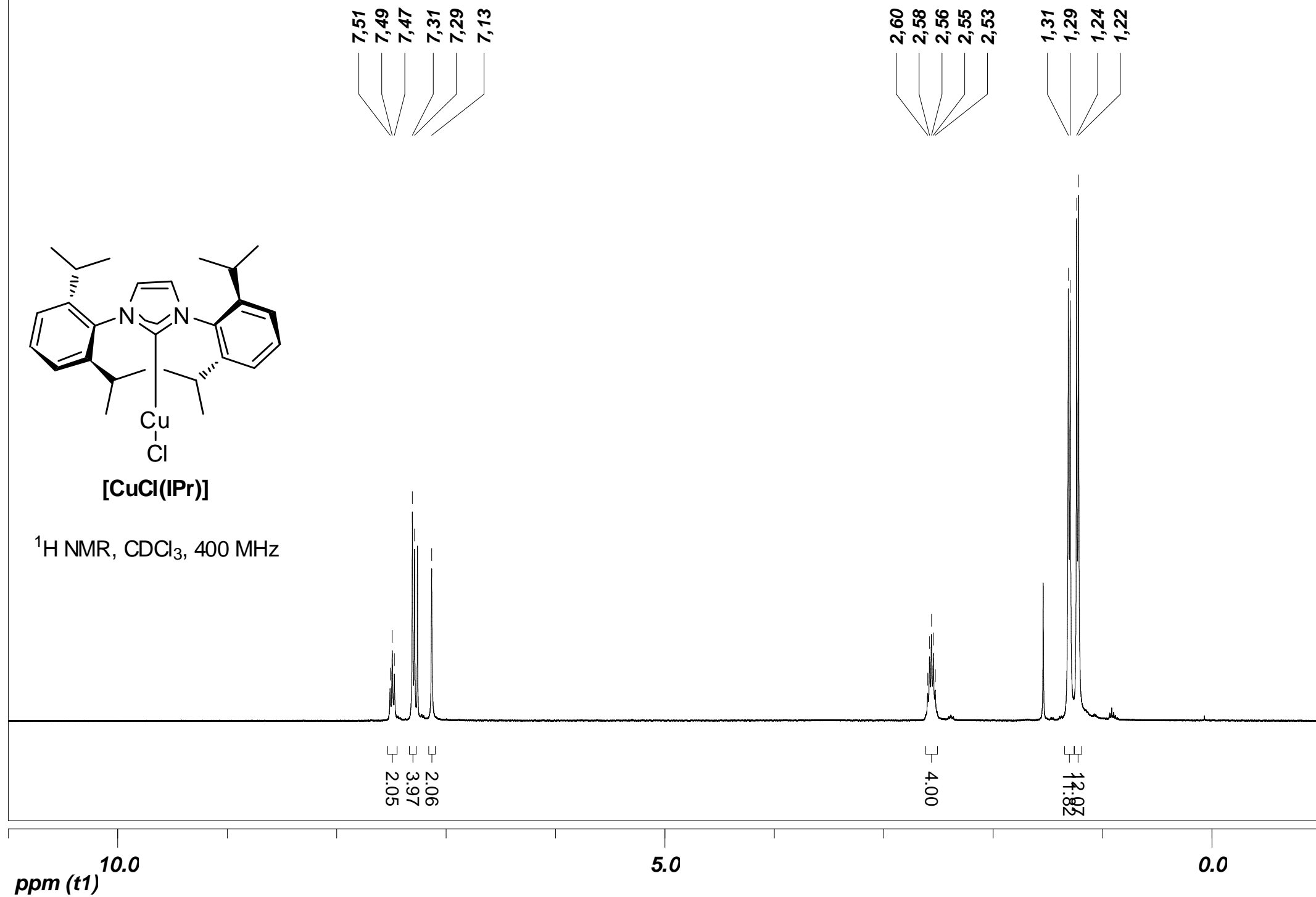
^1H NMR, CDCl_3 , 400 MHz

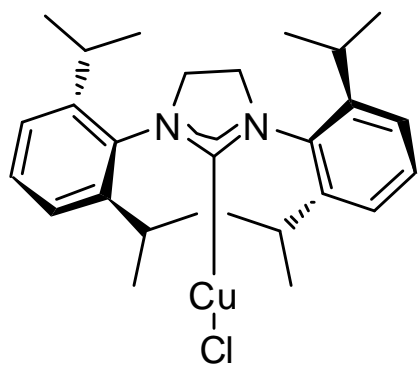




[CuCl(IPr)]

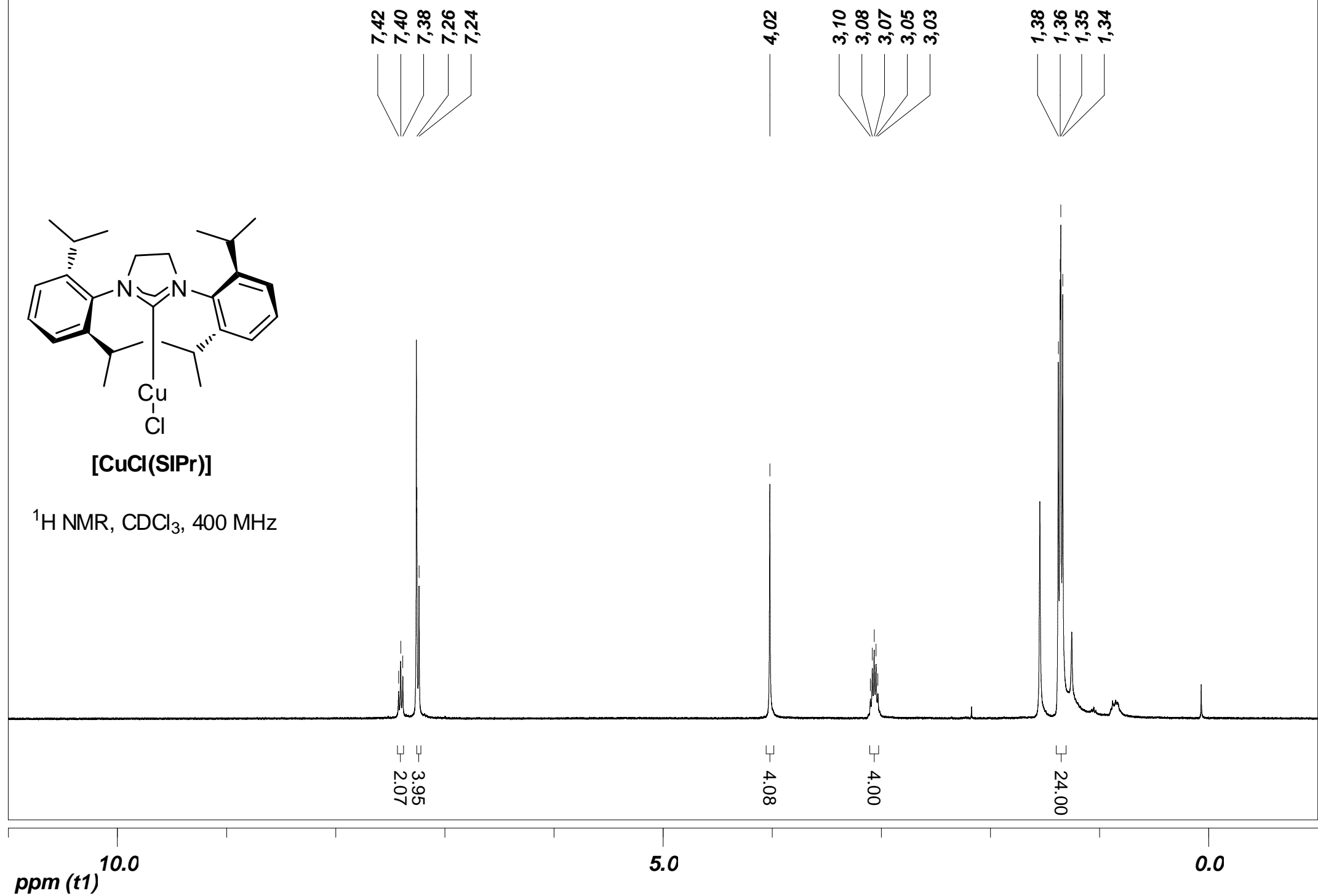
^1H NMR, CDCl_3 , 400 MHz

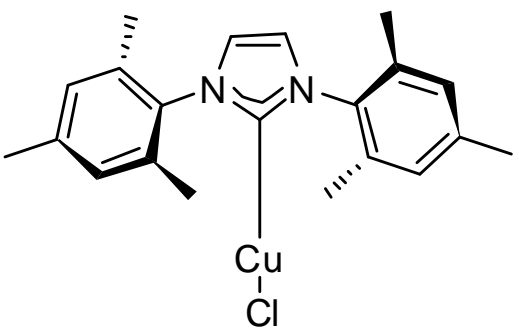




[CuCl(SiPr)]

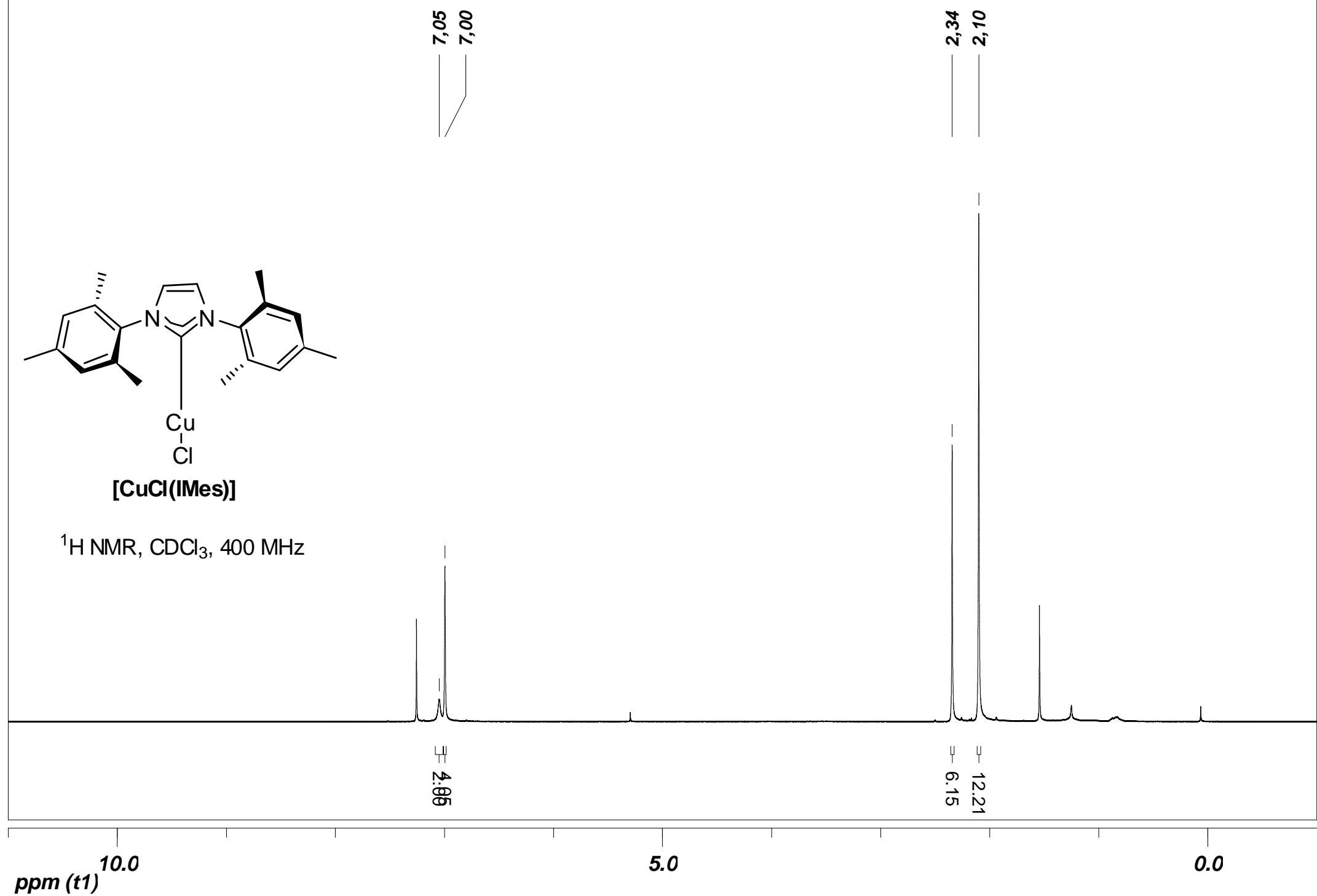
^1H NMR, CDCl_3 , 400 MHz

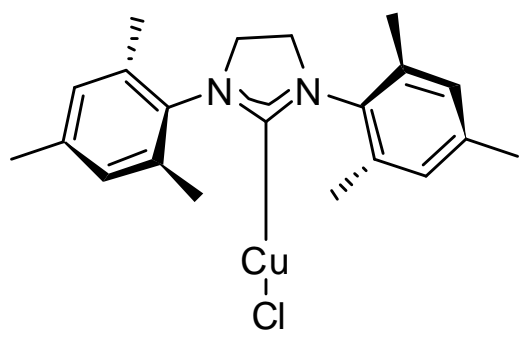




[CuCl(IMes)]

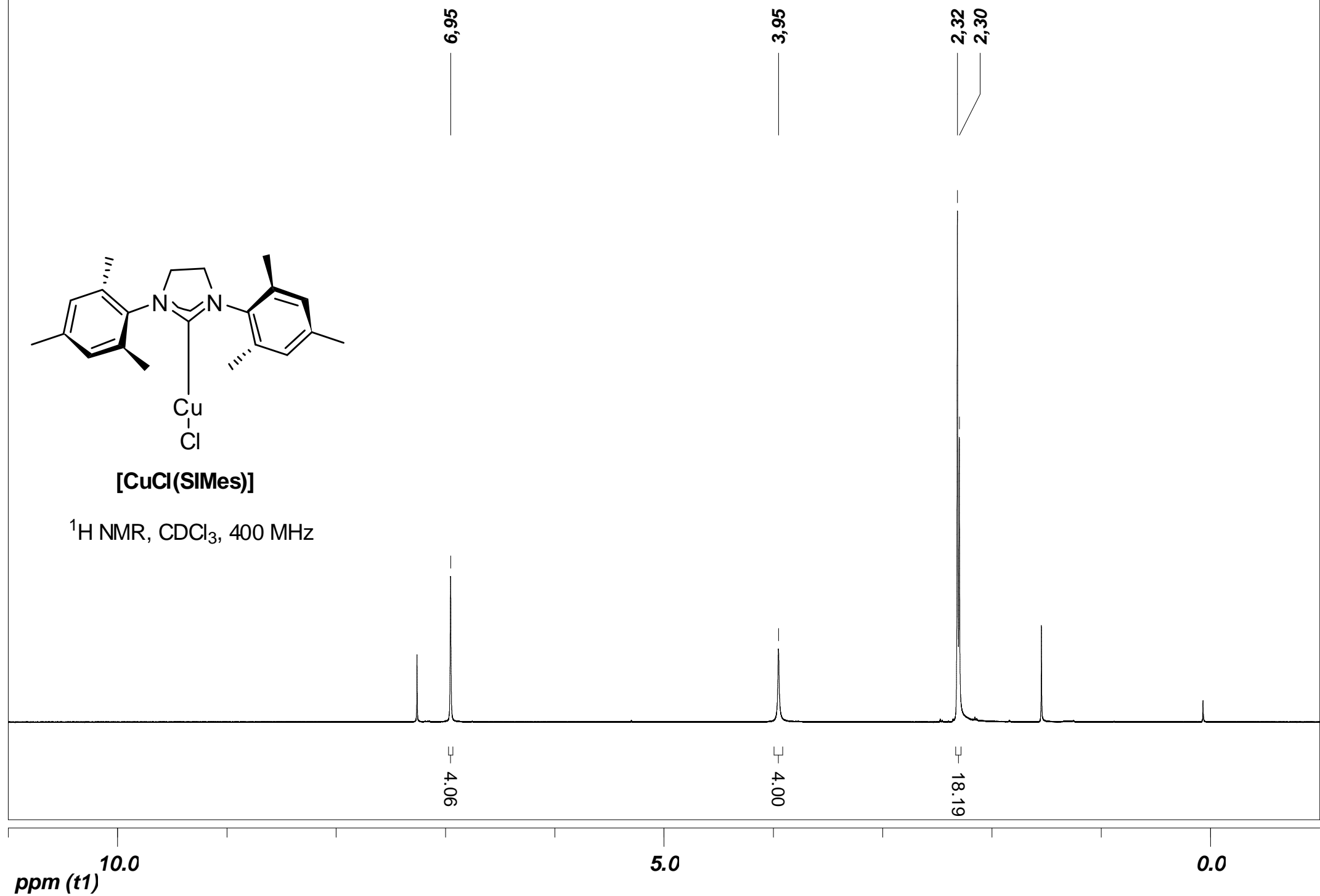
^1H NMR, CDCl_3 , 400 MHz

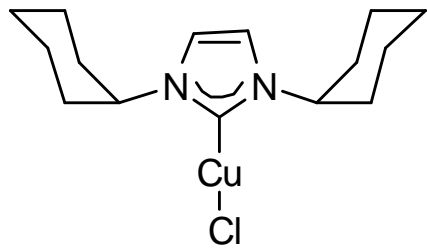




[CuCl(SIMes)]

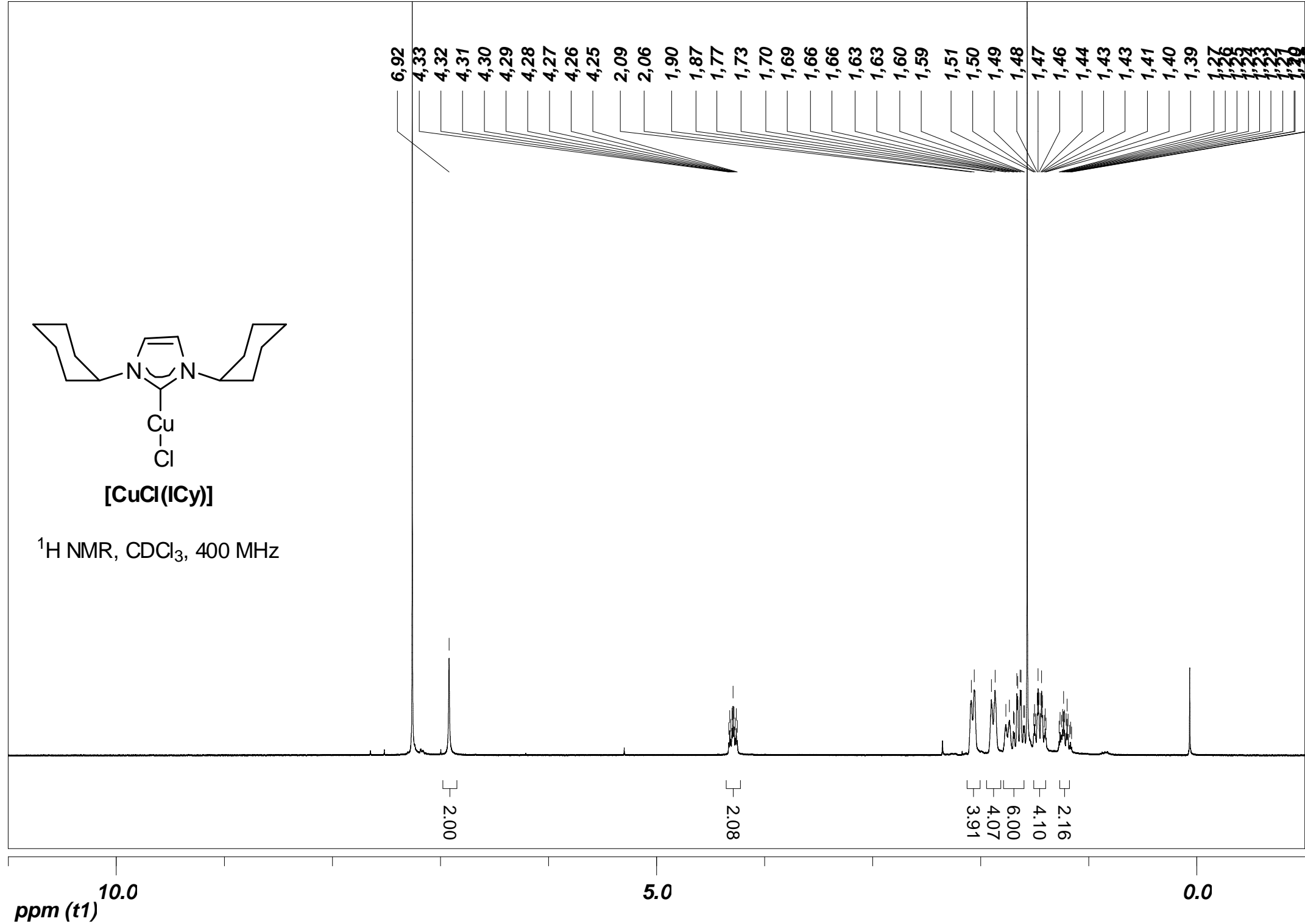
^1H NMR, CDCl_3 , 400 MHz

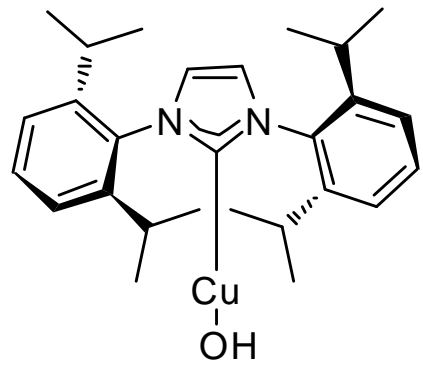




[CuCl(*ICy*)]

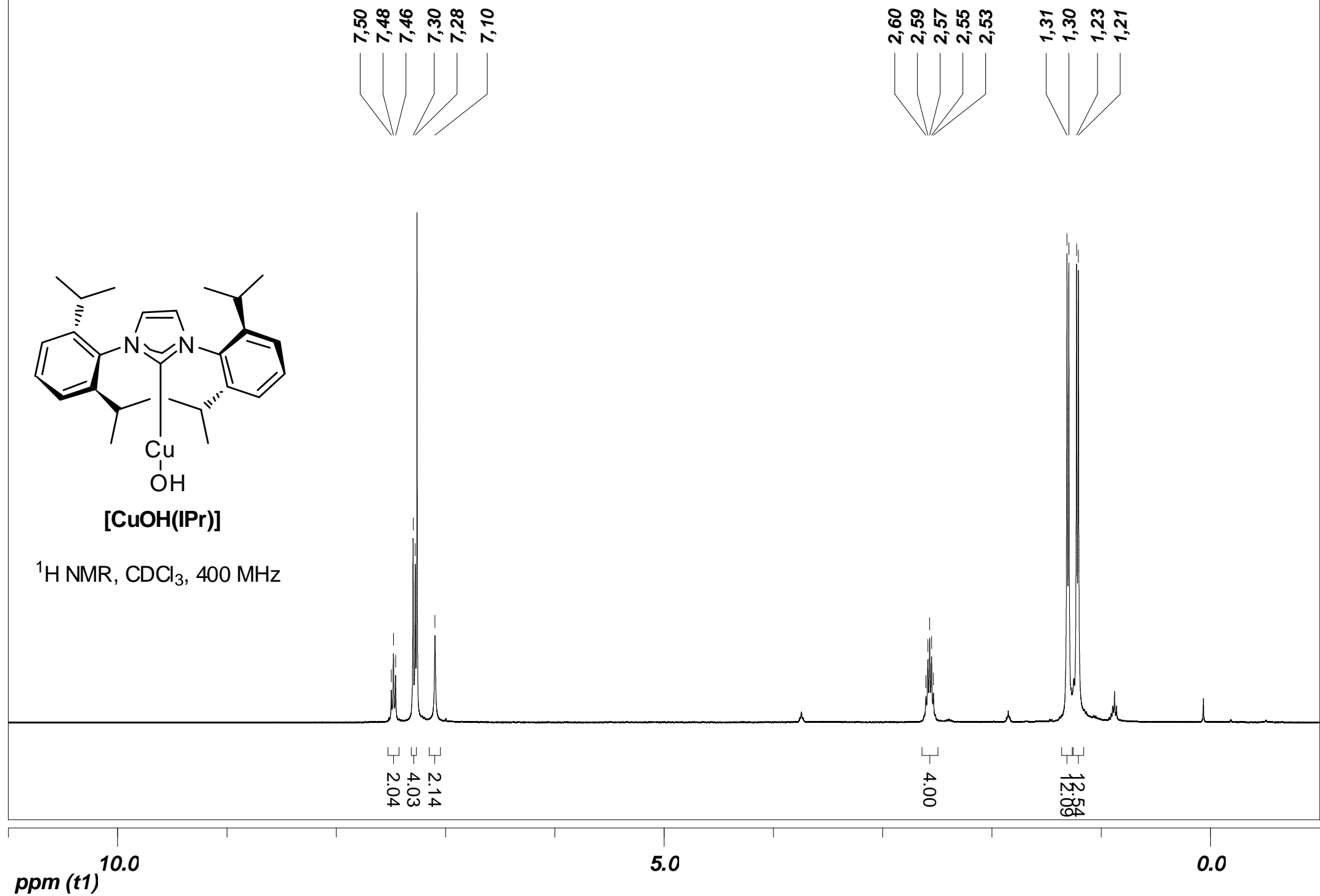
¹H NMR, CDCl₃, 400 MHz

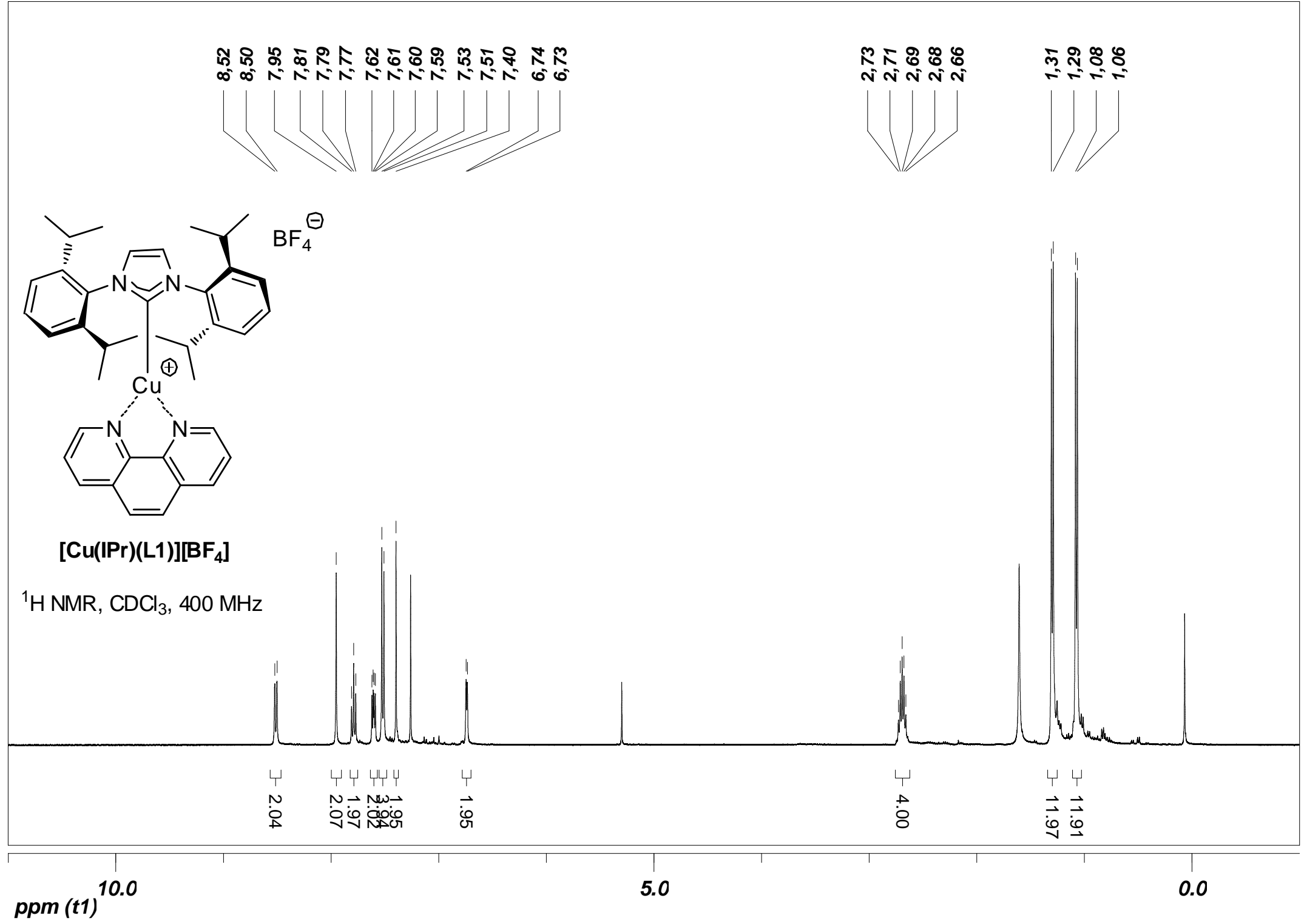


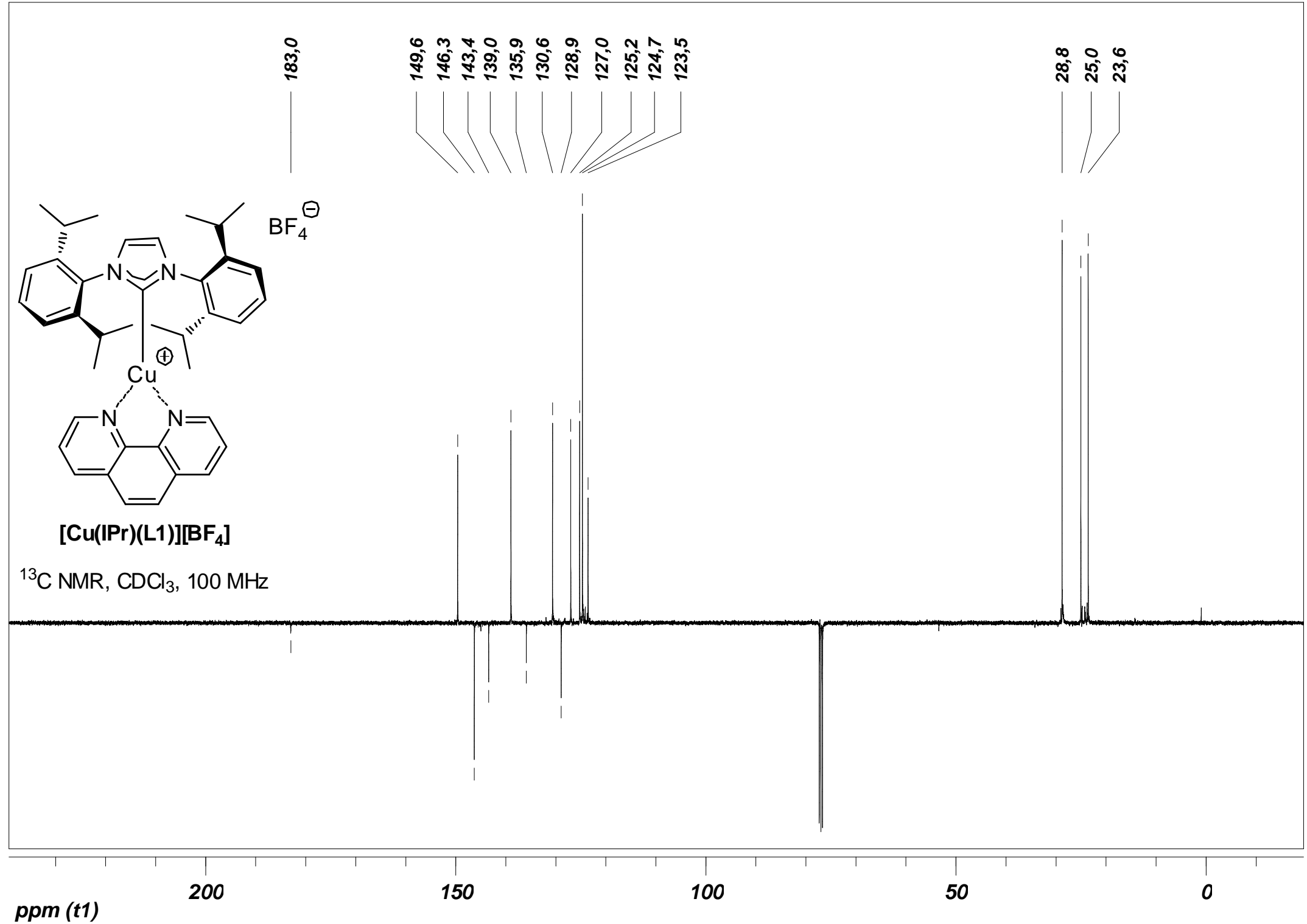


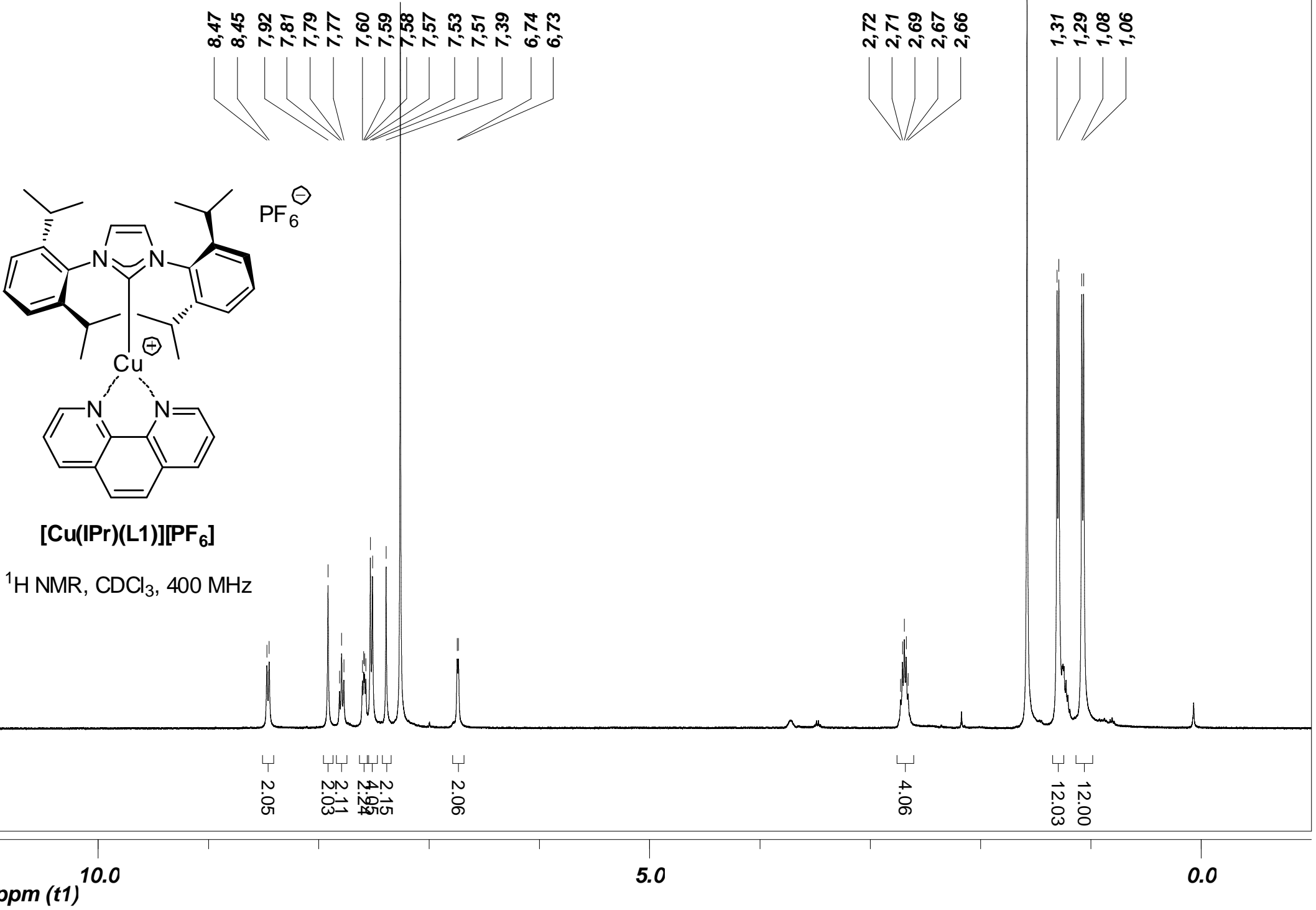
[CuOH(IPr)]

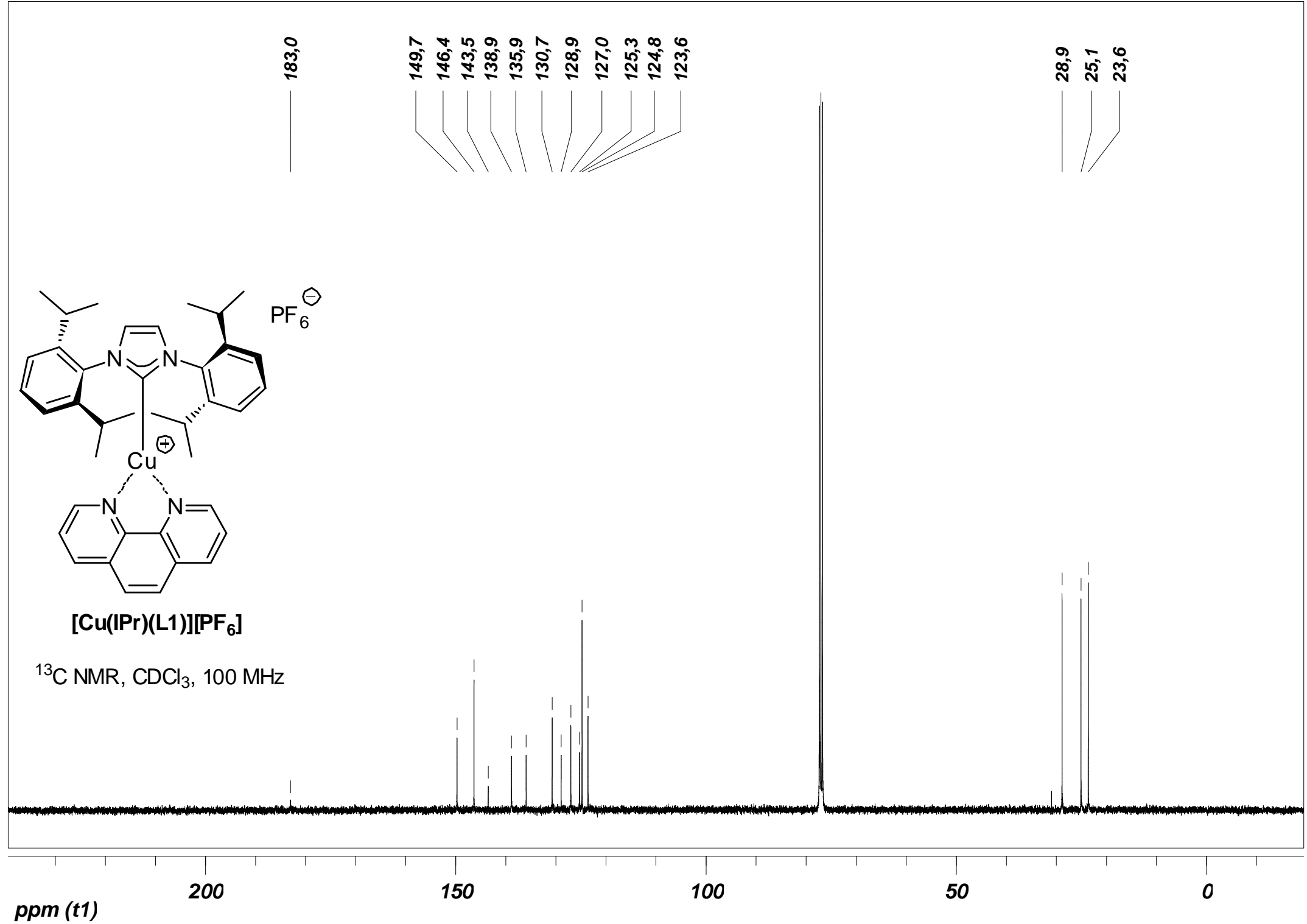
^1H NMR, CDCl_3 , 400 MHz

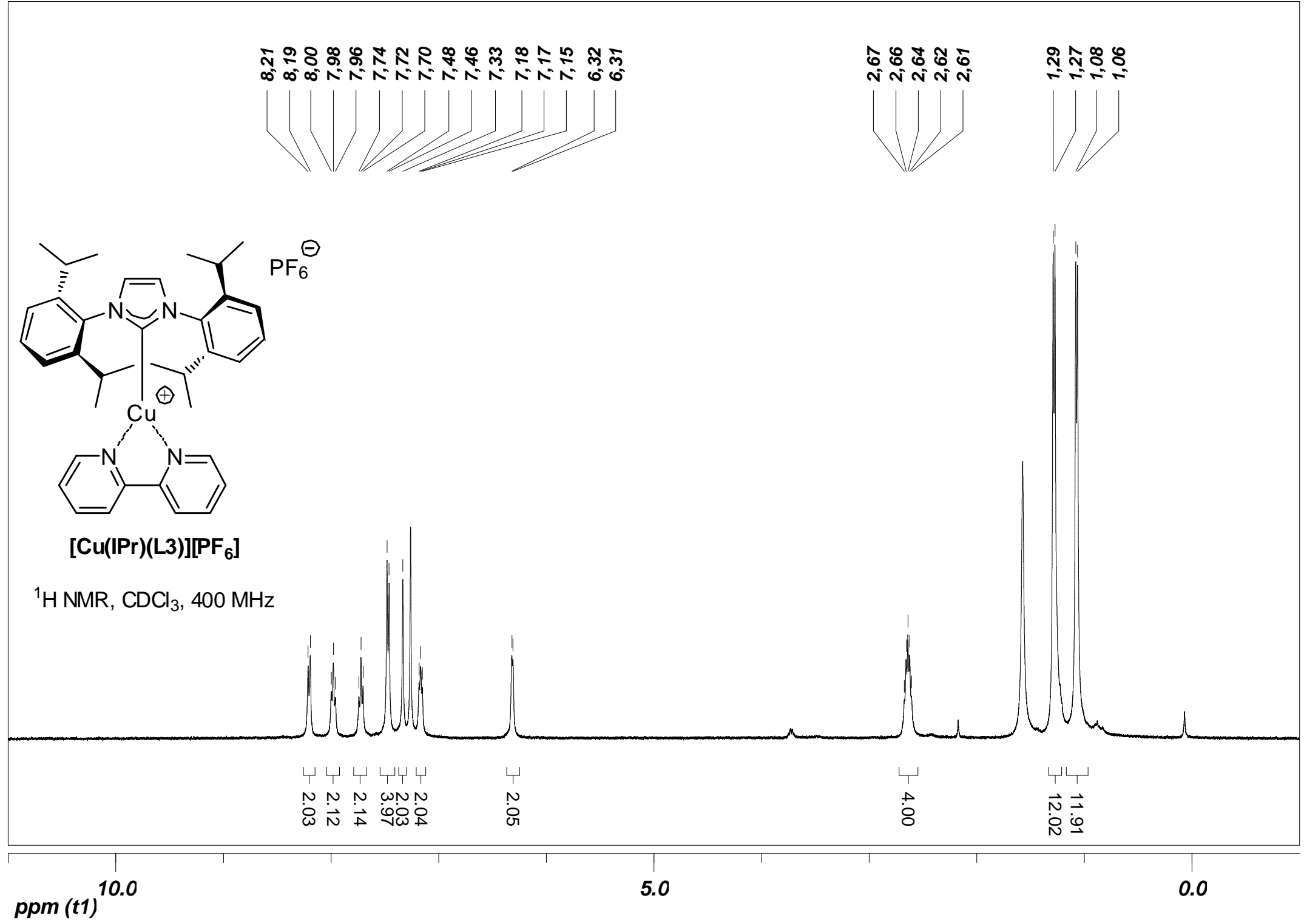








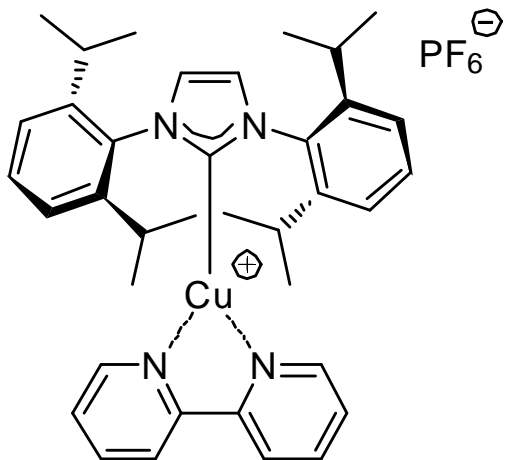




182,4

152,0
149,6
146,3
140,3
136,3
130,6
126,2
124,7
124,3
121,9

28,7
24,2
22,9



¹³C NMR, (CD₃)₂CO, 100 MHz

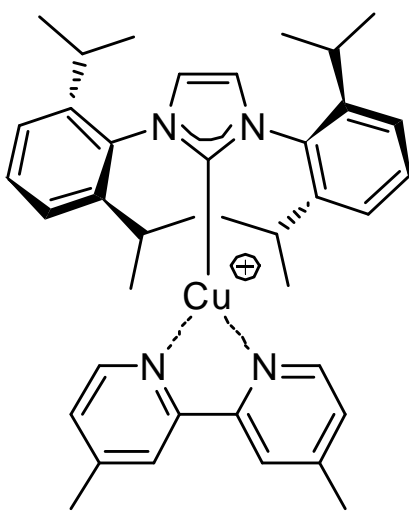
150

100

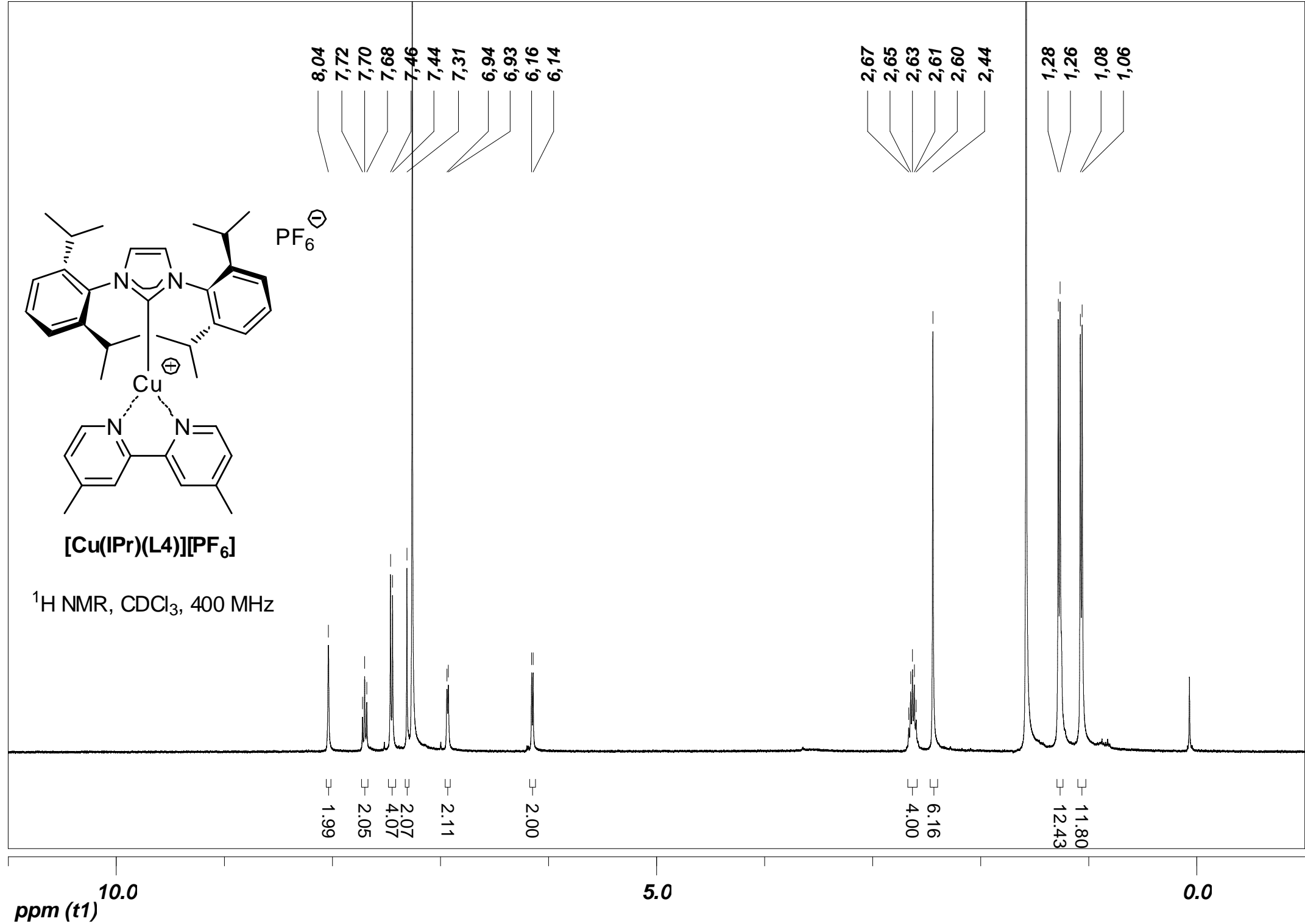
50

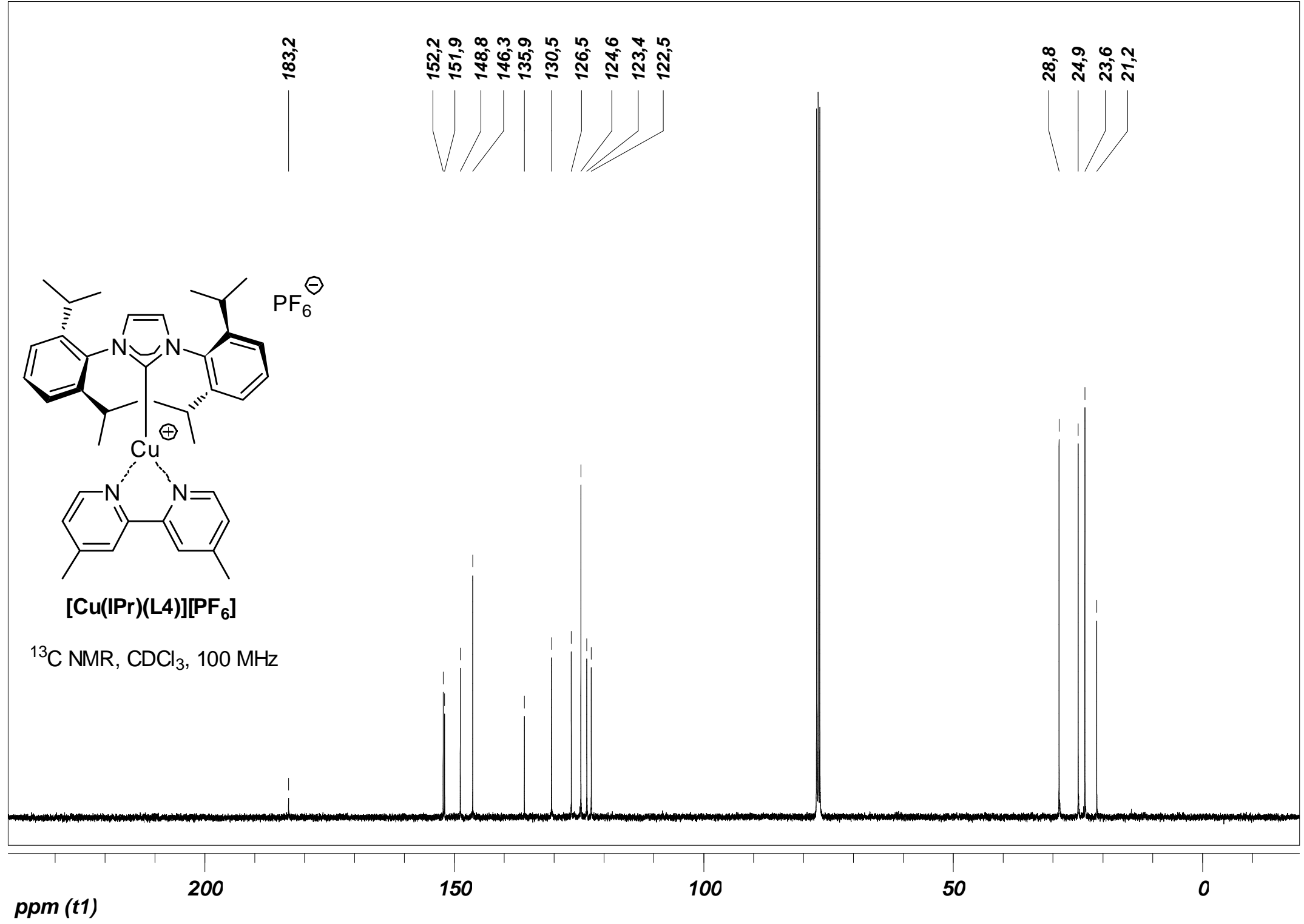
0

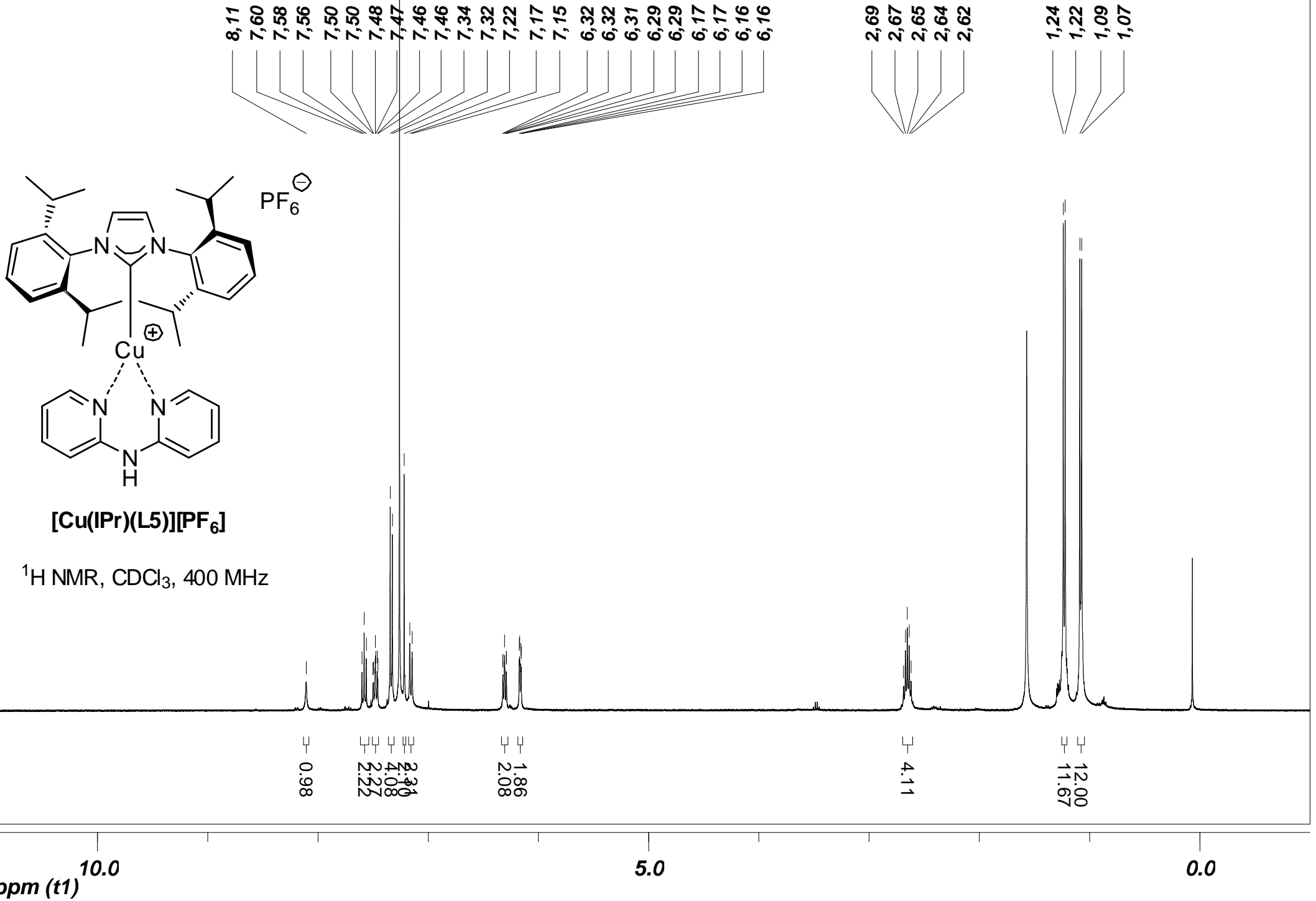
ppm (t1)

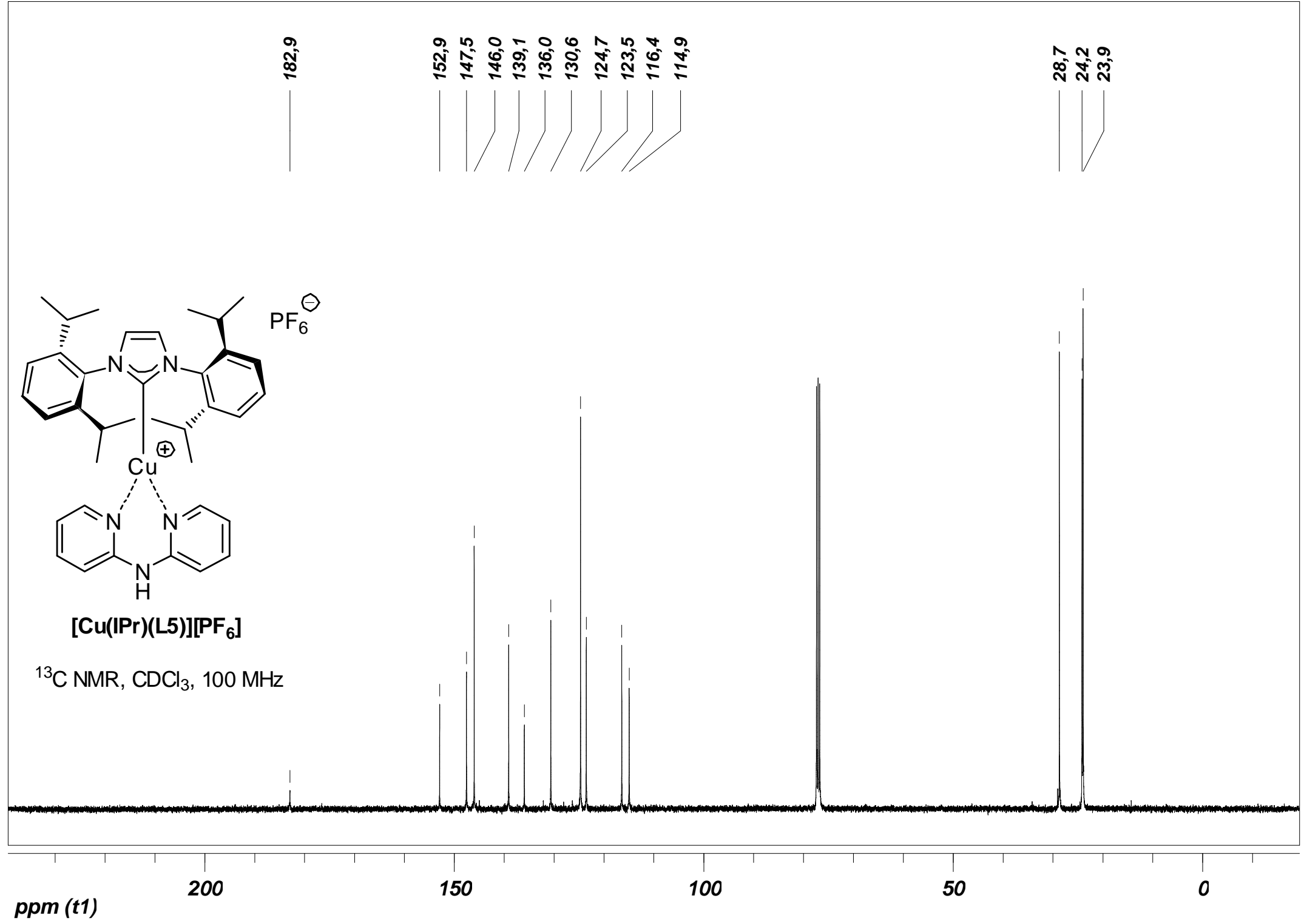


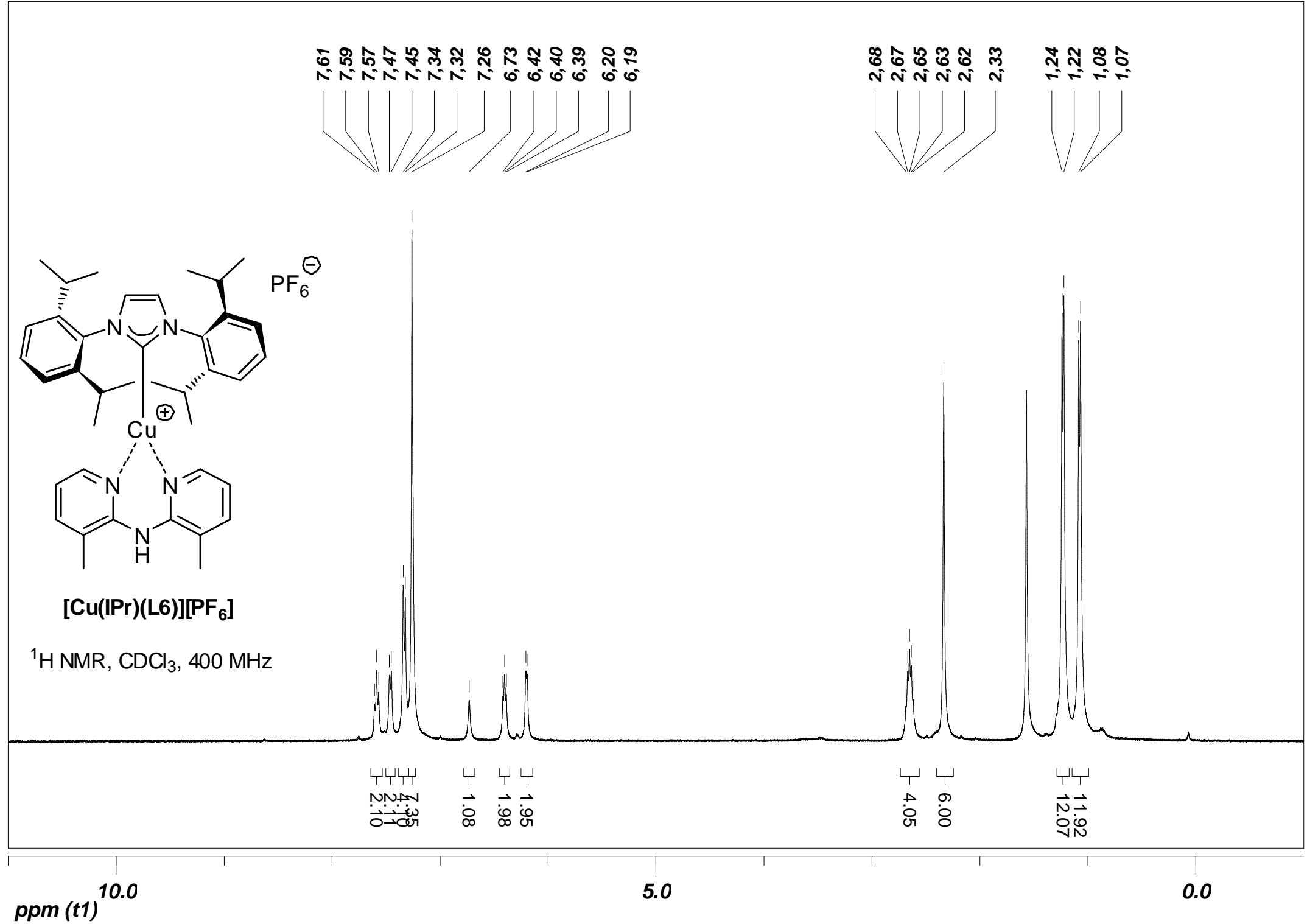
^1H NMR, CDCl_3 , 400 MHz

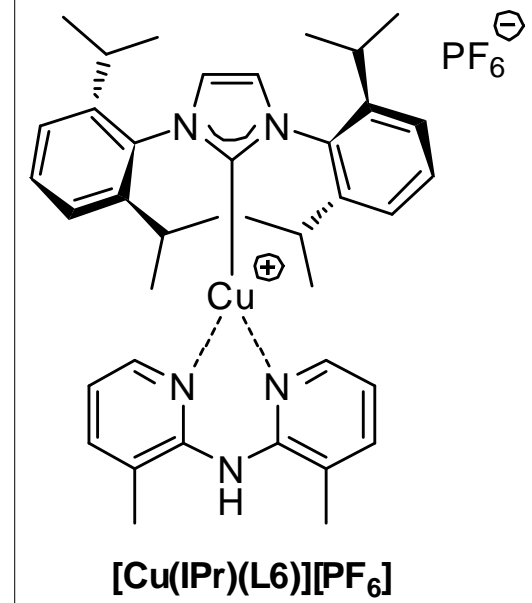




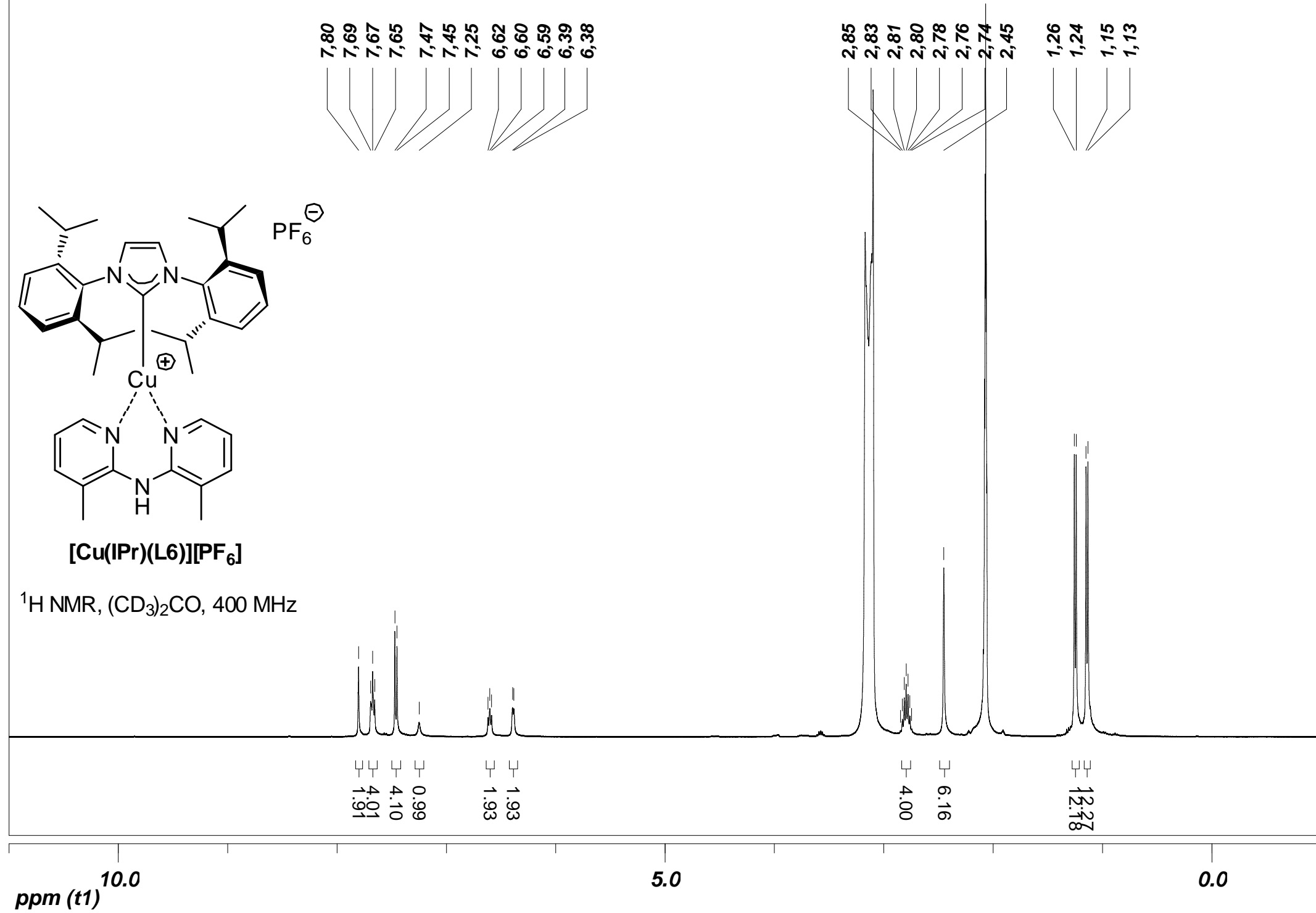


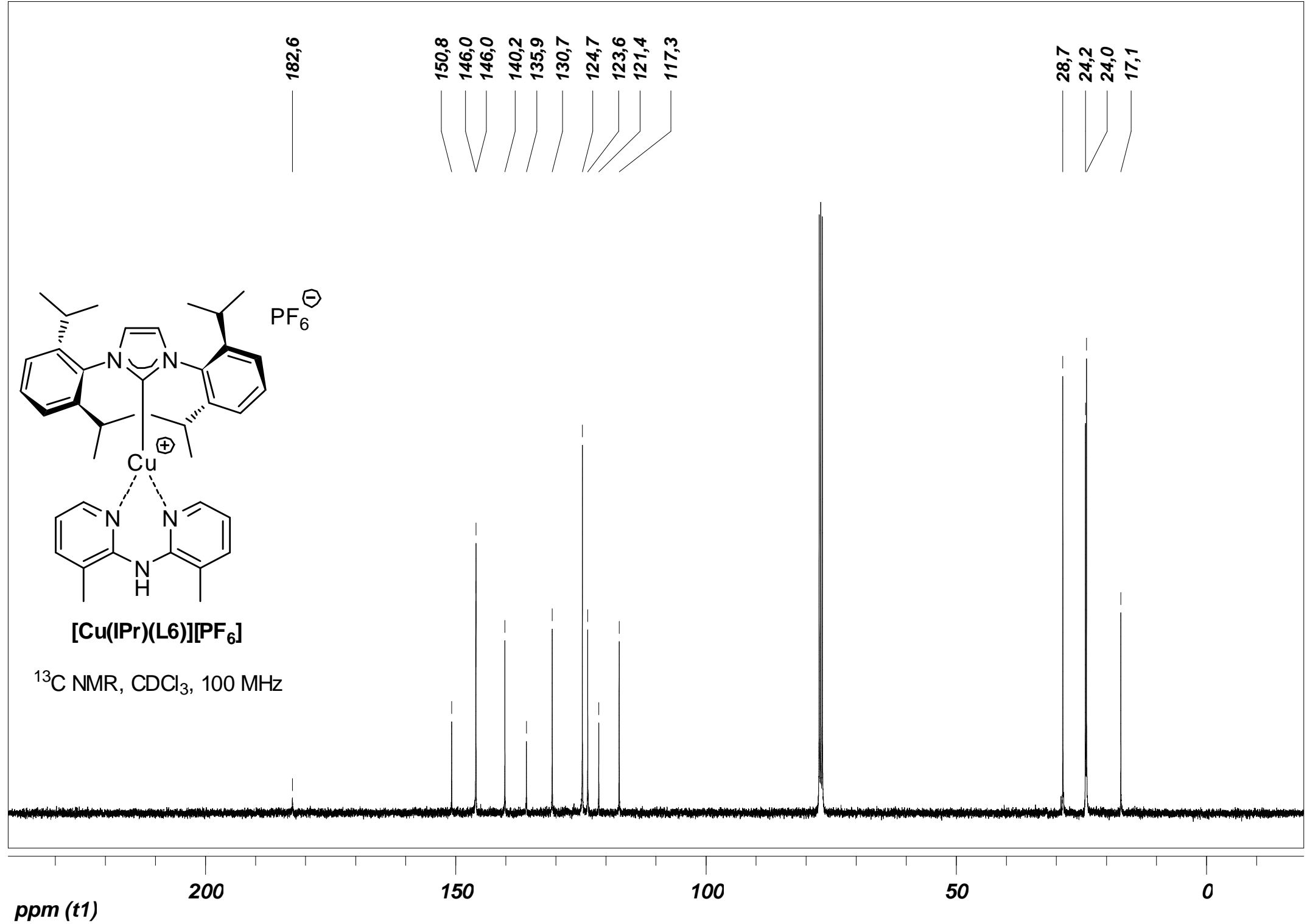


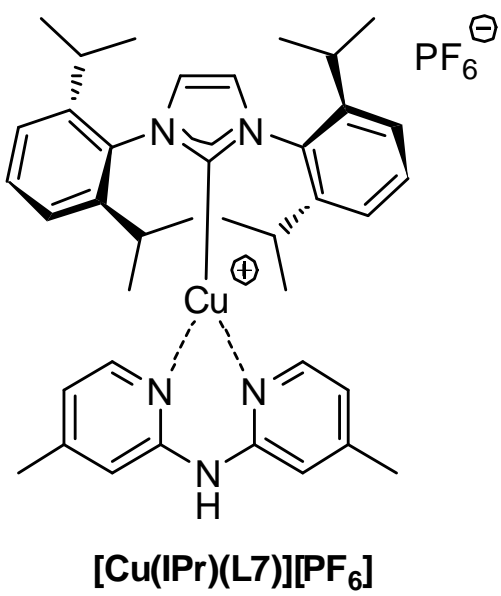




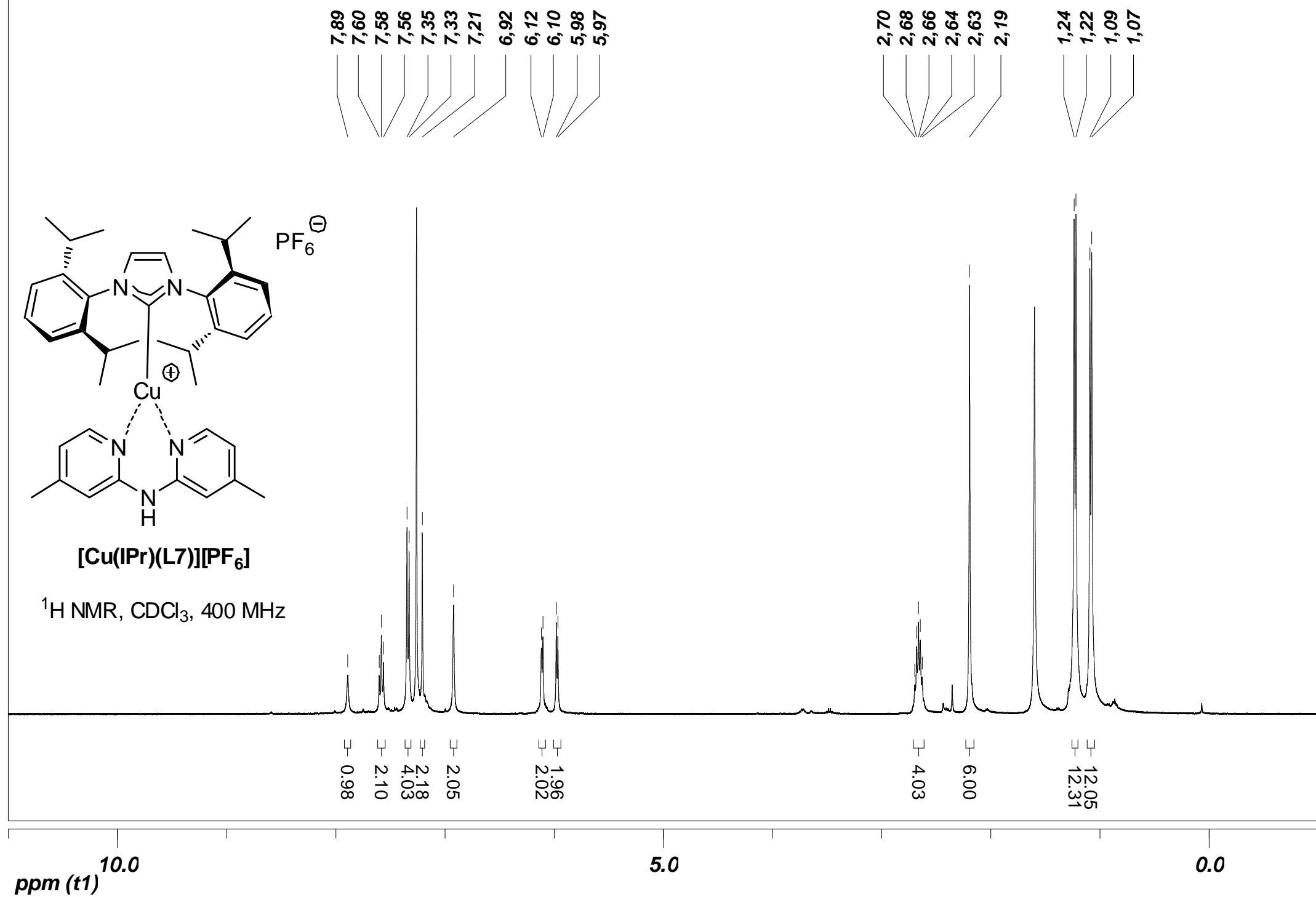
¹H NMR, (CD₃)₂CO, 400 MHz

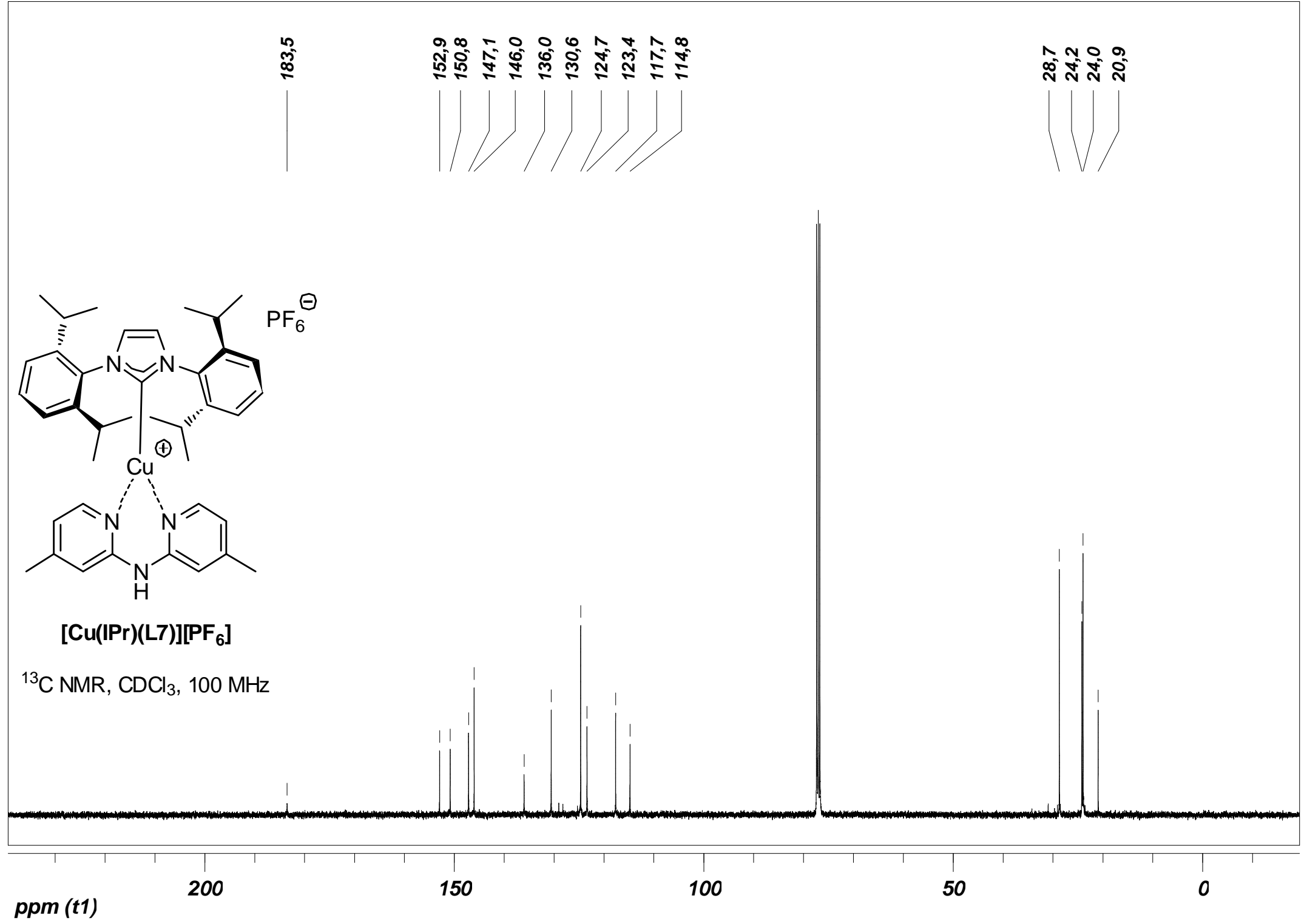


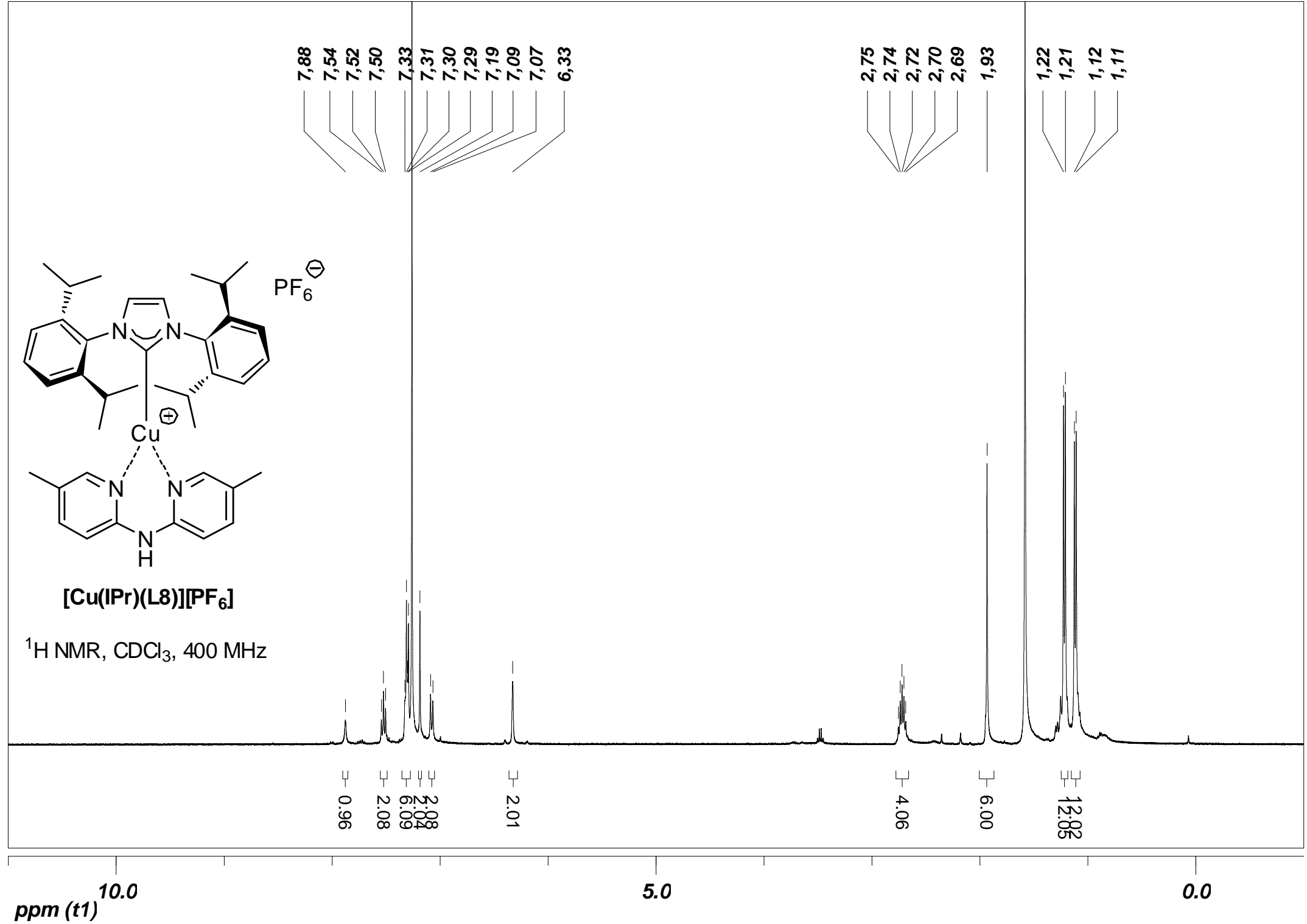


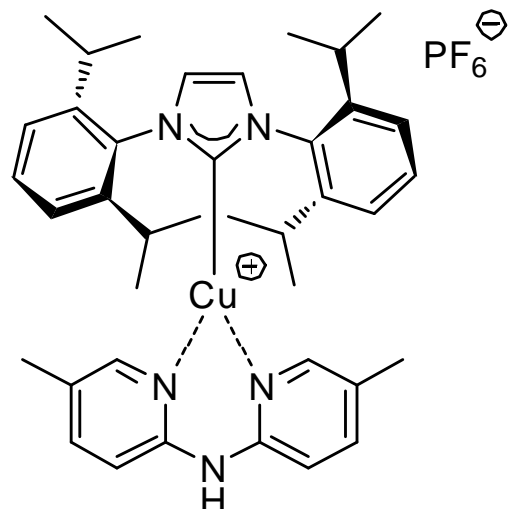


¹H NMR, CDCl₃, 400 MHz



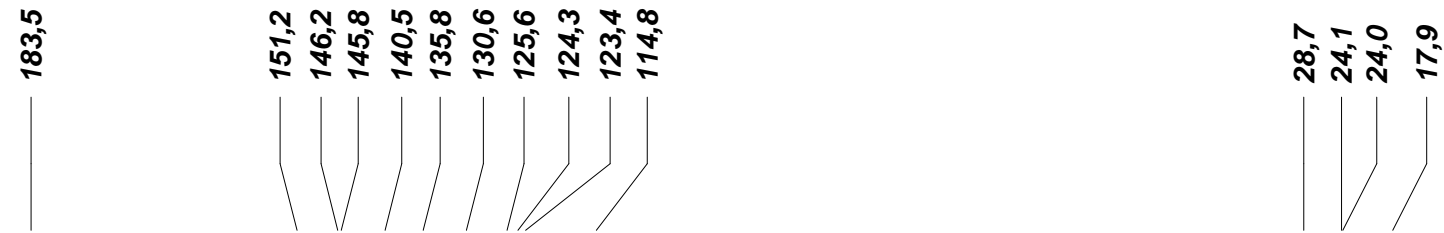






[Cu(IPr)(L8)][PF₆]

¹³C NMR, CDCl₃, 100 MHz



ppm (t1)

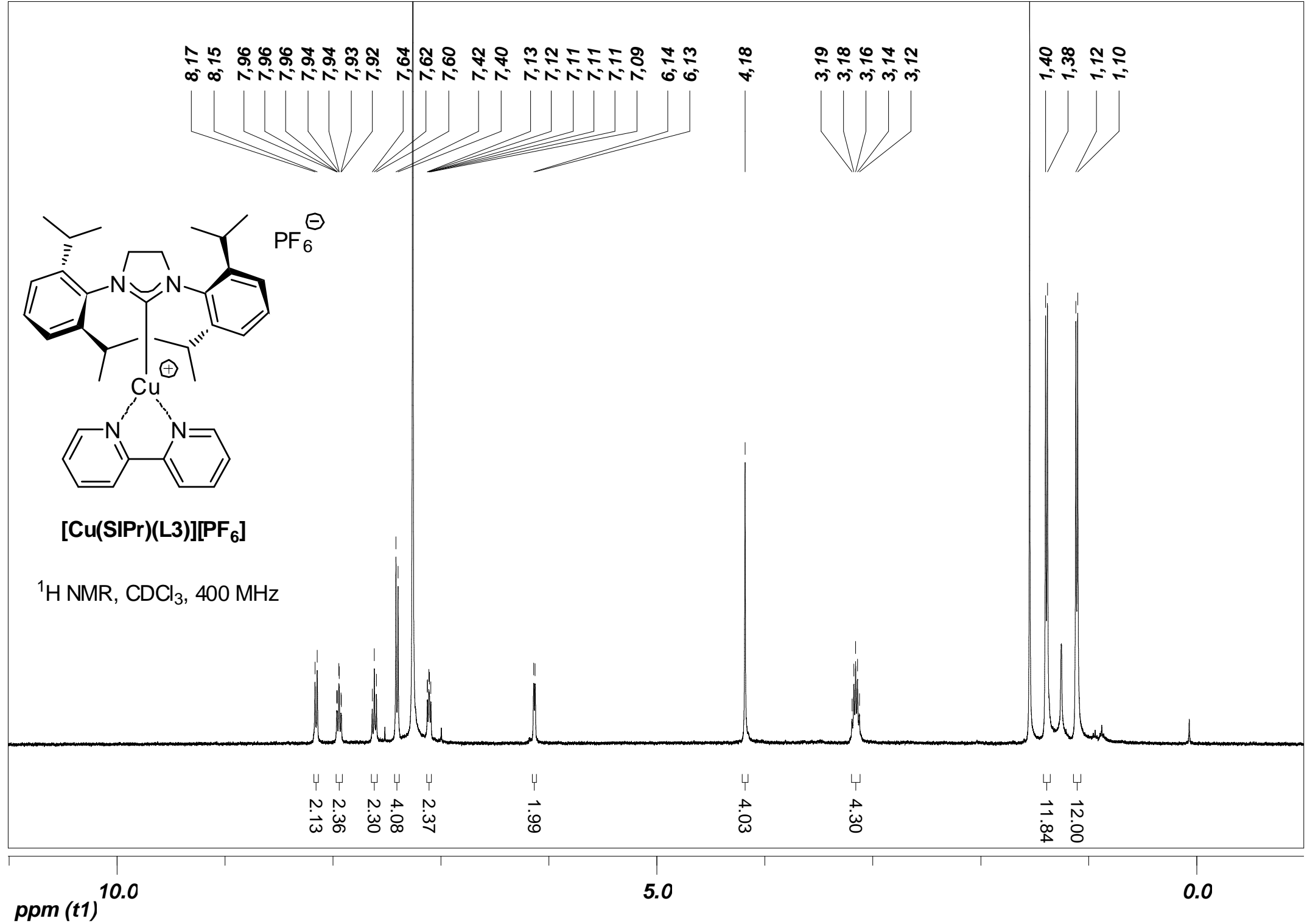
200

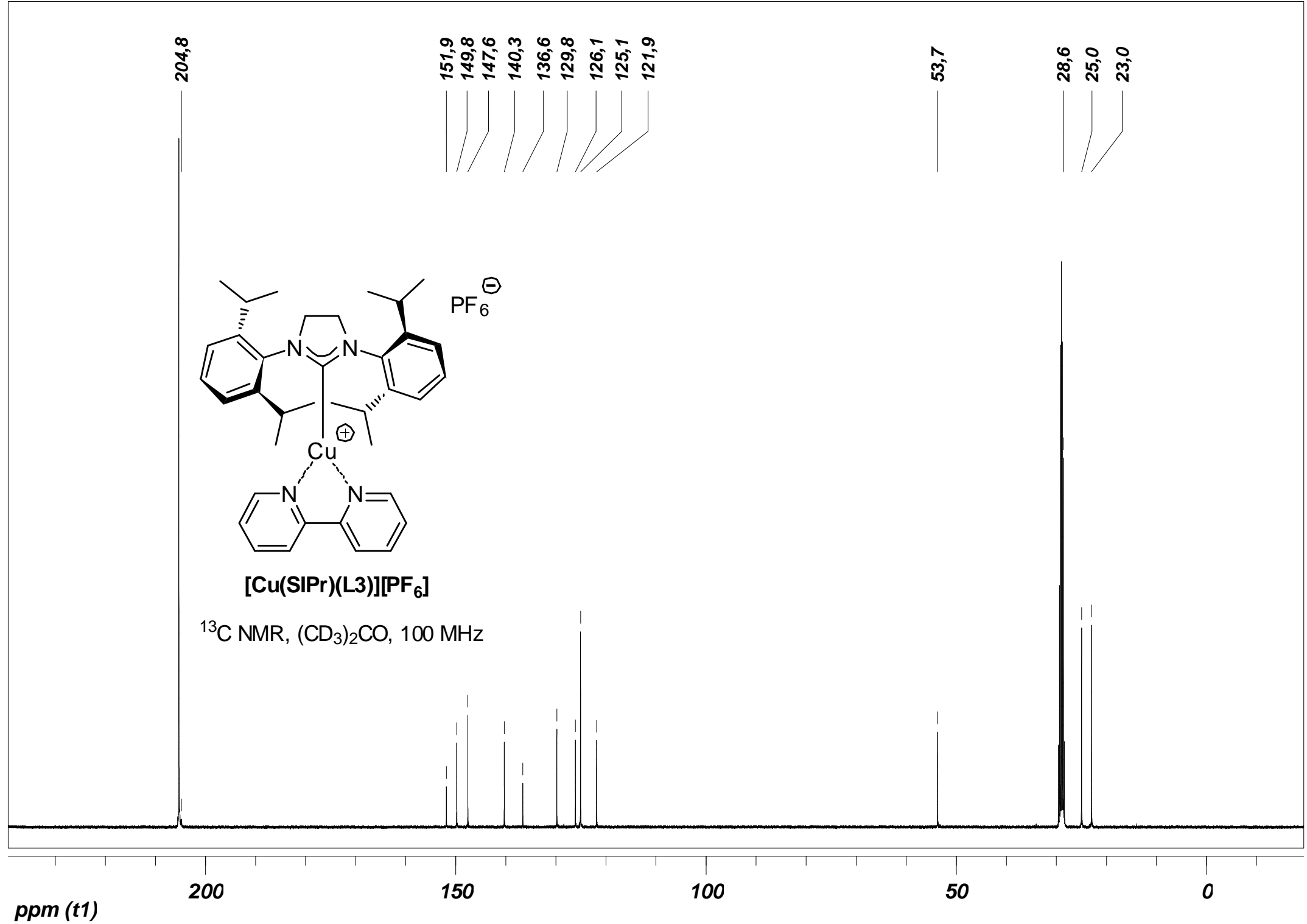
150

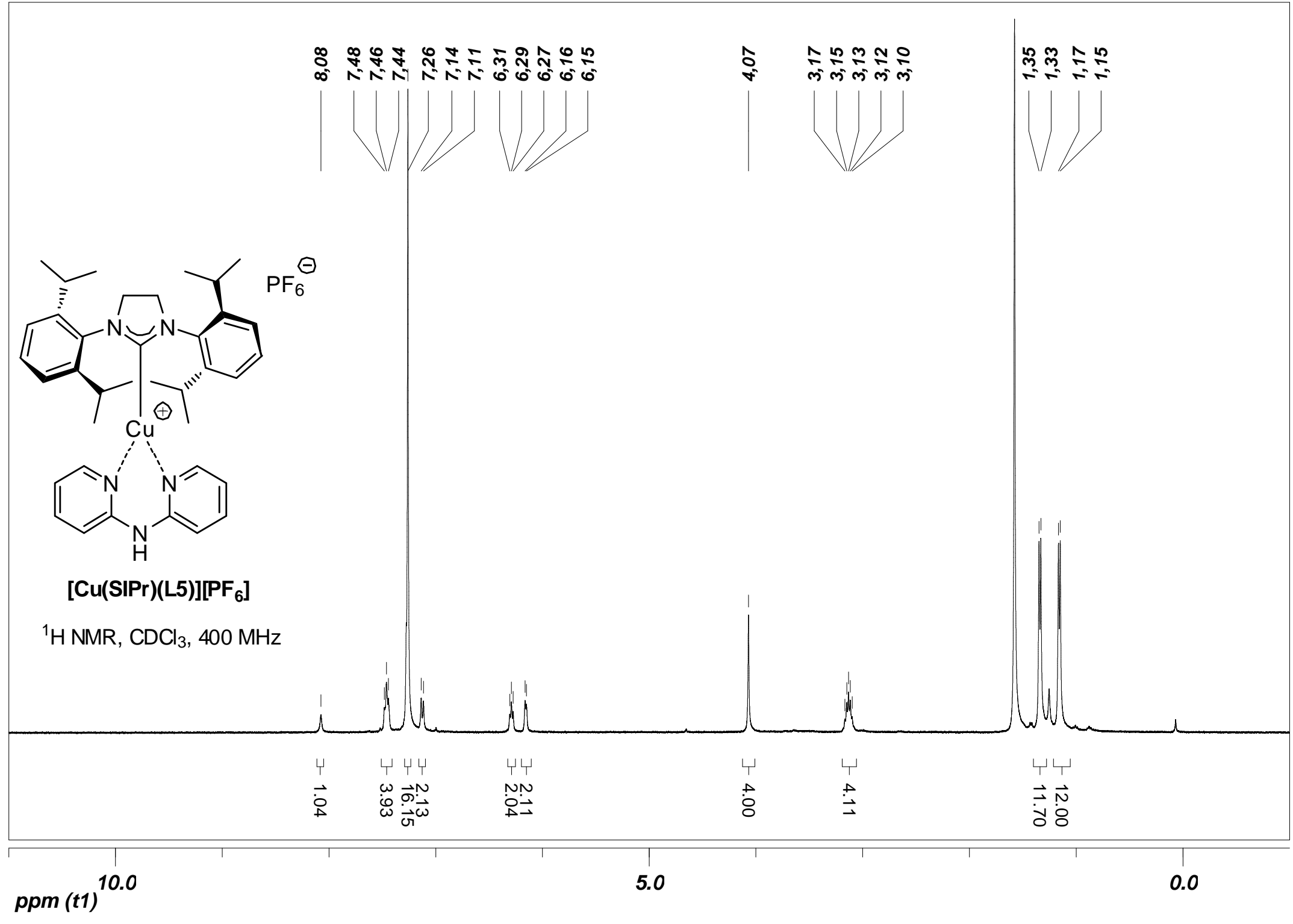
100

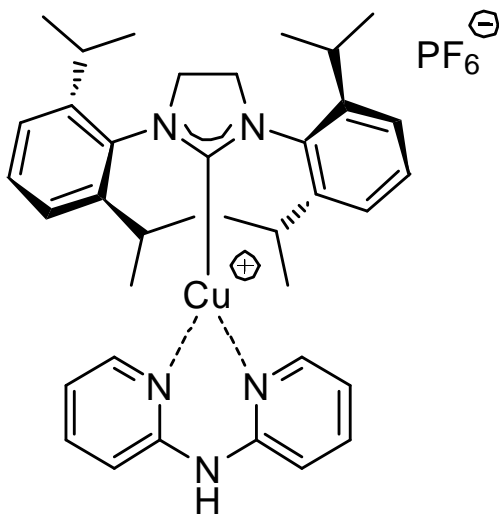
50

0



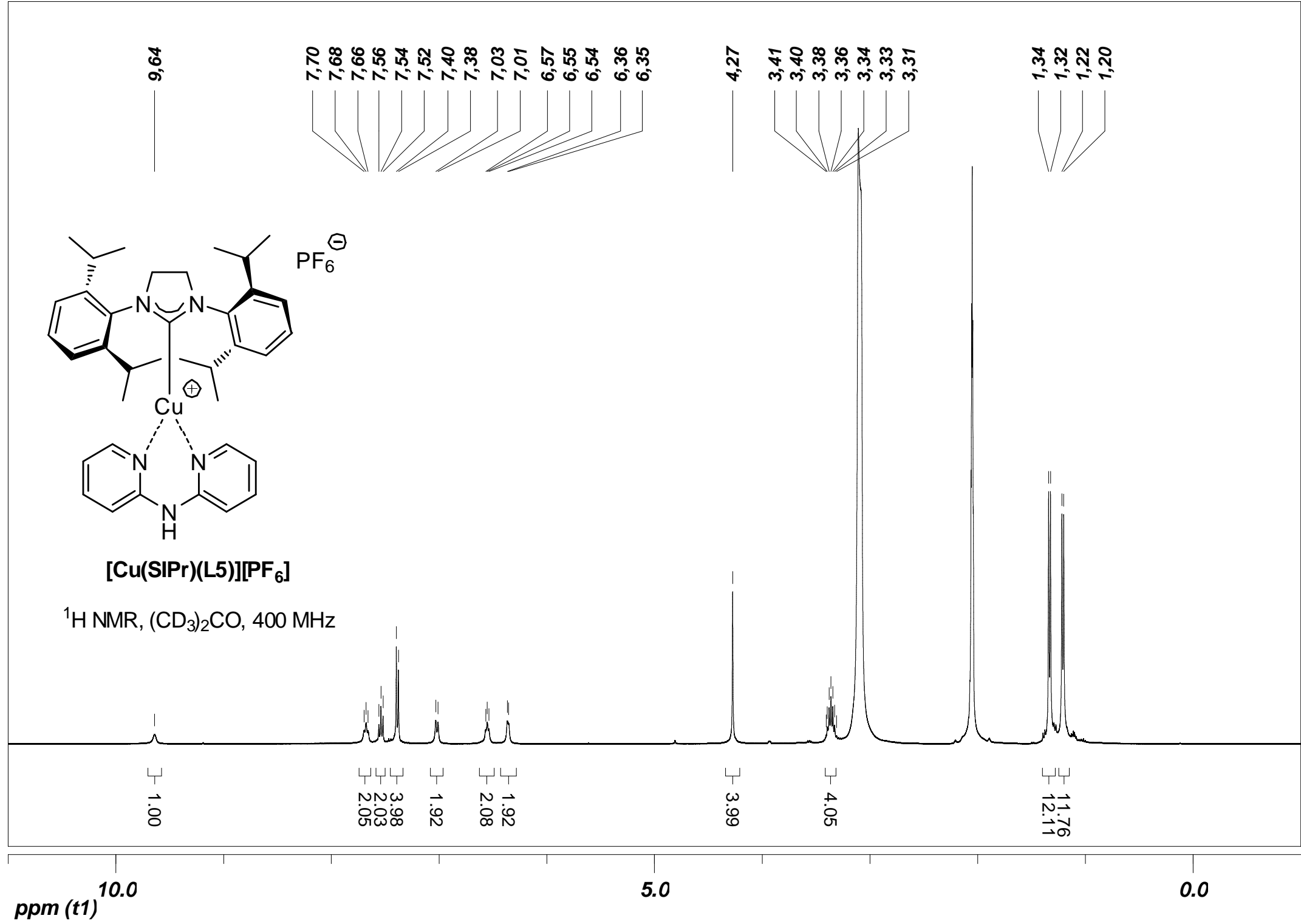


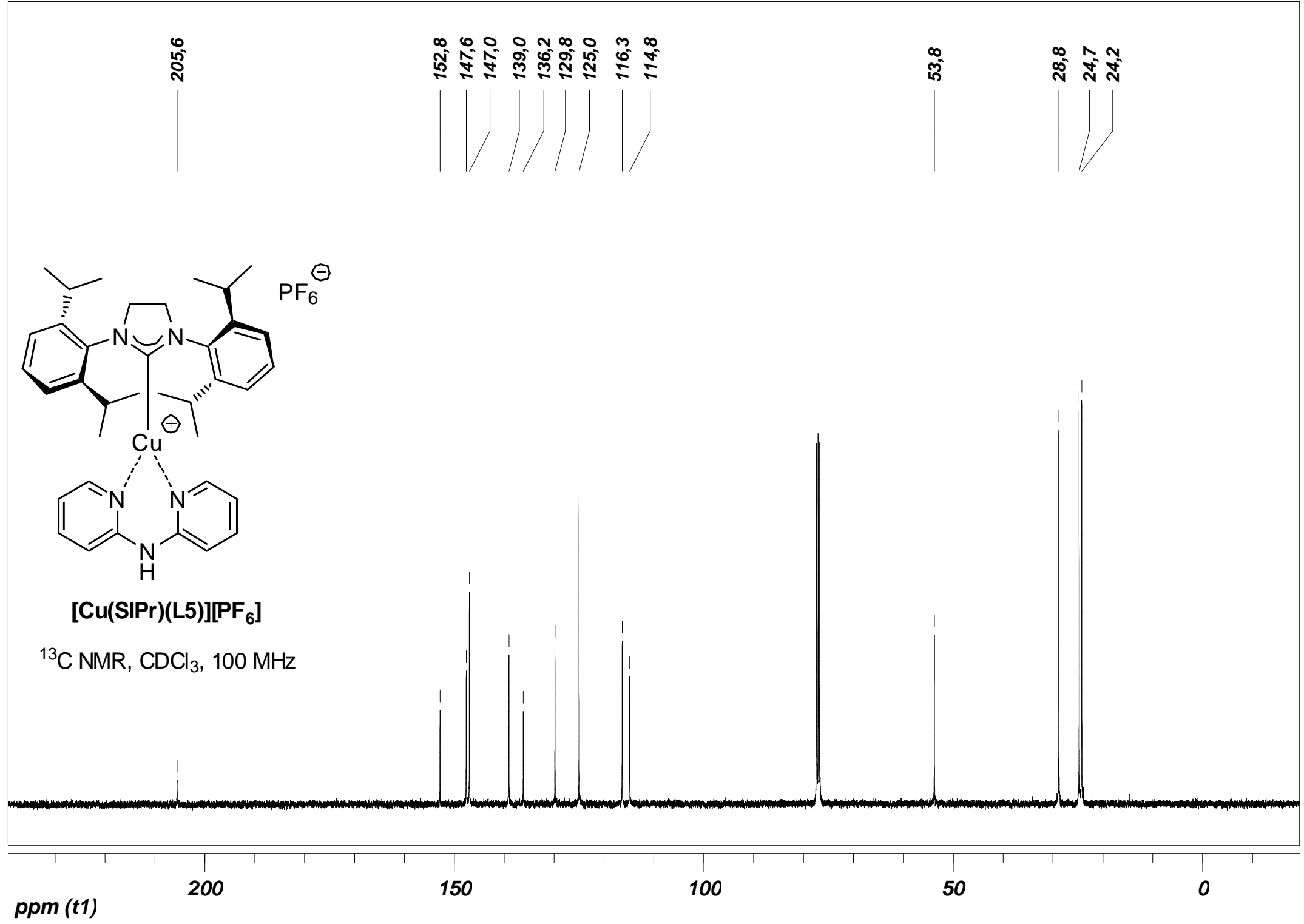


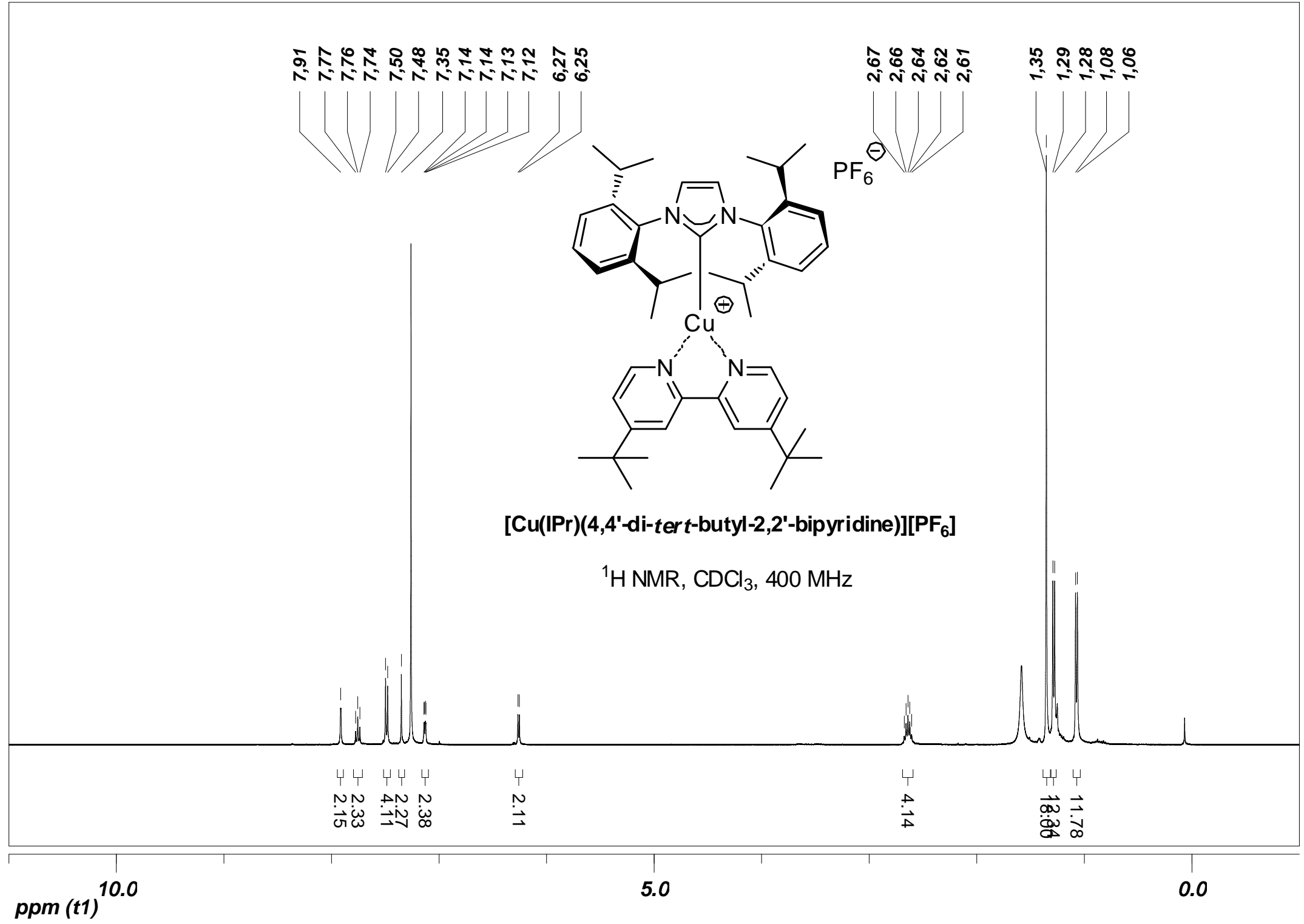


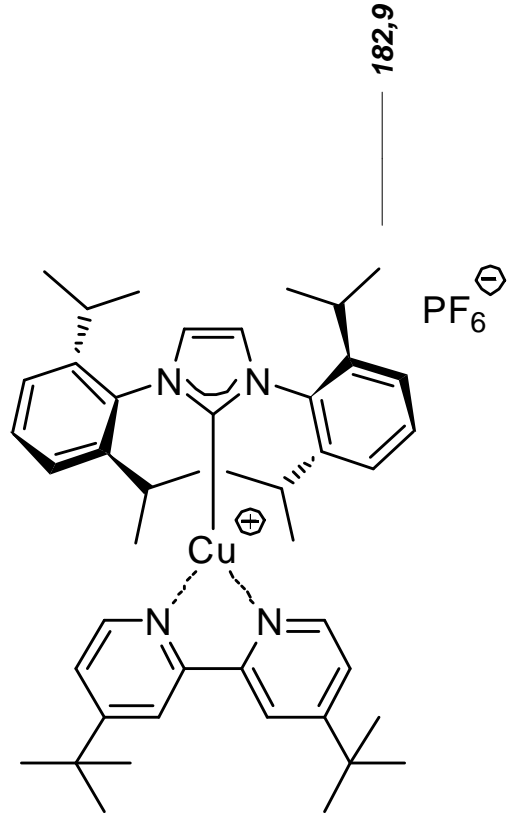
[Cu(SIPr)(L5)][PF₆]

¹H NMR, (CD₃)₂CO, 400 MHz









[Cu(IPr)(4,4'-di-*tert*-butyl-2,2'-bipyridine)][PF₆]

¹³C NMR, CDCl₃, 100 MHz

